AGT

Algebraic & Geometric Topology

Volume 25 (2025)

Highly twisted diagrams

Nir Lazarovich
Yoav Moriah
Tali Pinsky

msp

Algebraic & Geometric Topology **25**:1 (2025) 207–243
DOI: 10.2140/agt.2025.25.207
Published: 5 March 2025

Highly twisted diagrams

Nir Lazarovich
Yoav Moriah
Tali Pinsky

We prove that knots and links that have a 3-highly twisted irreducible diagram with more than two twist regions are hyperbolic. Furthermore, this result is sharp. The result is obtained using combinatorial techniques, using a new approach involving the Euler characteristic. By using geometric techniques, Futer and Purcell proved hyperbolicity under the assumption that the diagram is 6-highly twisted.

57K10, 57K32, 57K99

1 Introduction

The prevailing feeling among low dimensional topologists is that "complicated" links $\mathcal{L}$ in $\mathbb{S}^3$ are hyperbolic, ie the open manifold $\mathbb{S}^3 \setminus \mathcal{L}$ can be endowed with a complete, finite-volume, hyperbolic metric of sectional curvature -1. Being hyperbolic is a property of the manifold with far reaching consequences. However, proving that a specific link $\mathcal{L}$ is hyperbolic turns out to be nontrivial. This is especially true if the link $\mathcal{L}$ is "heavy duty", ie it has a very large crossing number. See for example Minsky and Moriah's work [12].

Our main theorem is:

Theorem A *Let $D(\mathcal{L})$ be a connected, prime, twist-reduced, 3-highly twisted diagram of a link $\mathcal{L}$ with at least two twist regions. Then $\mathcal{L}$ is hyperbolic.*

For the definitions see Section 2. Intuitively, being 3-highly twisted means that any crossing of the diagram is part of a sequence of at least 3 crossings of the same strings. For example, the diagram of the link in Figure 2 is 3-highly twisted. Clearly not all links have a diagram that satisfies the conditions of the theorem. However the subset of links that do is a "large" subset in a sense that can be made precise, see the discussion in [10] by Lustig and Moriah.

The assumption of being 3-highly twisted makes Theorem A *sharp* since there are nonhyperbolic links with 2-highly twisted link diagrams, as Figure 1 shows.

The question of when can one decide if the complement of a link in $\mathbb{S}^3$ is a hyperbolic manifold from a projection diagram has been of interest for a long time. The first result in this direction is by Hatcher and

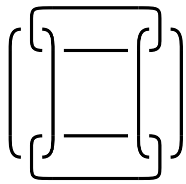

Figure 1: A nonhyperbolic link with a 2-highly twisted diagram.

Thurston [7] who proved that complements of 2-bridge knots which have at least two twist regions (they are not torus knots or links) are hyperbolic. The second is Menasco's result [11] that a nonsplit prime alternating link which is not a torus link is hyperbolic. Later Futer and Purcell proved in [4], among other results, that every link with a connected, prime, twist-reduced, 6-highly twisted diagram which has at least two twist regions is hyperbolic. Two other relevant results are by Giambrone [5] and by Futer, Kalfagianni and Purcell [3], in which the condition that the diagram is 6-highly twisted is replaced by conditions related to its "semiadequacy" (as defined there).

Theorem A, which is proved using combinatorial techniques, weakens the conditions imposed by Futer and Purcell [4] on $D(\mathcal{L})$ from 6-highly twisted to 3-highly twisted. Their result is obtained by applying geometric bounds, using Lackenby's 6-surgery theorem, see [8], to the corresponding fully augmented links. The fact that combinatorial techniques can be used to improve on geometric bounds is not surprising and was repeatedly demonstrated in the study of three manifolds, for example in work by Culler, Gordon, Luecke and Shalen [2], Gordon and Luecke [6] and Li [9].

We believe that the methods used in this paper are interesting in themselves, and could be used in studying other problems. For example, as a corollary to Theorem A we obtain a simple method to construct essential surfaces in complements of links with highly twisted diagrams. This is stated in Section 7 as Theorem B.

Although there are nonhyperbolic links with 2-highly twisted diagrams, we expect that the 3-highly twisted condition can be weakened to generalize Theorem A to a larger class of links which includes alternating links (cf [11]).

Outline of the proof

By Thurston [14], it suffices to show that the link complement has incompressible boundary, and is irreducible, atoroidal and unannular. These can be formulated as the nonexistence of an essential surface S of nonnegative Euler characteristic. Given an essential surface S in the link complement, consider its curves of intersection $\mathcal{C}$ with the projection plane P. To each curve $c \in \mathcal{C}$ we assign its "contribution" to the Euler characteristic $\chi_+(c)$ and show that $0 \le \chi(S) = \sum_{c \in \mathcal{C}} \chi_+(c)$ (see Lemma 4.2). In general there might be curves $c \in \mathcal{C}$ with $\chi_+(c) > 0$. Given such a curve, the 3-highly twisted condition forces the existence of neighboring curves with negative χ_+. This allows us to redistribute the Euler characteristic among the curves by defining for each $c \in \mathcal{C}$ a modified Euler characteristic $\chi'(c)$ so that $0 \le \chi(S) = \sum_{c \in \mathcal{C}} \chi'(c)$ and $\chi'(c) \le 0$ (see Lemmas 5.15 and 5.16). This shows that $\chi(S) \le 0$. Moreover, we get that $\chi'(c) = 0$ for all $c \in \mathcal{C}$. A case by case analysis then shows that all curves must be of a particular form (see Definition 6.3 and Propositions 6.7 and 6.13) from which it follows that S must be a boundary parallel torus.

Acknowledgments

Lazarovich was supported by the Israel Science Foundation (grant 1562/19). The authors thank the anonymous referee for helpful comments.

2 Preliminaries

2.1 Bubbles and twist regions

Let $\mathcal{L} \subset \mathbb{S}^3$ be a link. The projection of a link L in the isotopy class $\mathcal{L}$ onto a plane P together with the crossing data is a *link diagram* of L and is denoted by $D(L)$. Let ε be sufficiently small so that the closed ε-balls around the crossings of $D(L)$ are disjoint. Let $\mathcal{B}_1, \dots, \mathcal{B}_r$ be ε-balls around the r crossings of the diagram. The boundaries $B_i = \partial \mathcal{B}_i$, $1 \le i \le r$, are the *bubbles* of the diagram. The link $\mathcal{L}$ is isotopic to a link L which is embedded in $P \cup \bigcup_i B_i$. Note that P divides each bubble into two hemispheres denoted by B_i^+ and B_i^-. Denote the two 2-spheres

$$P^{\pm} = \left(P \smallsetminus \bigcup_i \mathcal{B}_i \right) \cup \bigcup_i B_i^{\pm}.$$

Each of P^+, P^- bounds a 3-ball $H^{\pm}$ in $\mathbb{S}^3 \smallsetminus L$.

A *twist region* T is a disk in P which contains a maximal (with respect to inclusion) chain of bigons in $D(L)$ describing a trivial integer 2-tangle. See Figure 2 for an example of a diagram with twist regions. We will assume that a twist region contains the projection of the bubbles around the crossings in T. We

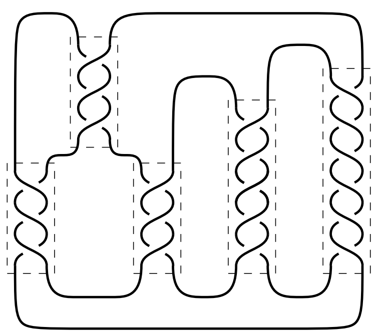

Figure 2: A 3-highly twisted link diagram. The twist regions are the dashed rectangles.

will often abuse terminology, and use twist regions to refer to the regions in $P^{\pm}$ which project to twist regions. Correspondingly, we treat the bubbles around the crossings of T as being contained in T. A *twist box* is the tangle $(\boldsymbol{T}, t)$ where $\boldsymbol{T}$ is the product $T \times [-2\varepsilon, 2\varepsilon]$ for a twist region T, and t is the tangle $\boldsymbol{T} \cap L$. The diagram $D(L)$ uniquely decomposes into disjoint twist regions.

Definition 2.1 Let $D(L)$ be a link diagram.

(1) The diagram $D(L)$ is *prime* if any simple closed curve in P intersecting $D(L)$ transversely in two points bounds a subdiagram with no crossings.

(2) A *twist-reduction subdiagram* is a subdiagram of $D(L)$ enclosed by a simple closed curve γ in P which intersects $D(L)$ transversely in four points composed of two pairs each of which is adjacent to a crossing of $D(L)$ but which is not a chain of bigons describing an integer 2-tangle. The diagram $D(L)$ is *twist-reduced* if it contains no twist-reduction subdiagram.

(3) For $k \in \mathbb{N}$, the diagram is k*-highly twisted* if every twist region has at least k crossings.

Note that every diagram can be made twist-reduced by performing flypes on twist-reduction subdiagrams.

Definition 2.2 A twist region T intersects the link diagram in four points, dividing its boundary ∂T into four segments. If the twist region has at least two crossings, then a pair of opposite segments of ∂T can be called the *length edge* or *width edge* of T as in

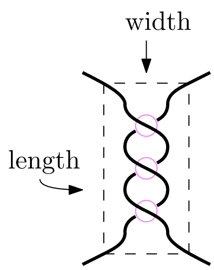

3 Surfaces in link complements

3.1 Normal position

We are interested in studying compact surfaces S properly embedded in $\mathbb{S}^3 \smallsetminus \mathcal{N}(L)$. If $\partial S \neq \varnothing$ we extend S by shrinking the neighborhood $\mathcal{N}(L)$ radially. This determines a map $\iota\colon (S, \partial S) \to (\mathbb{S}^3, L)$, whose image we denote by S as well, which is an embedding on the interior of S.

Lemma 3.1 *Let $S \subset \mathbb{S}^3 \smallsetminus \mathcal{N}(L)$ be a proper surface with no meridional boundary components, and let $(\boldsymbol{T}, t)$ be a twist box. Then, up to isotopy, $S \cap \boldsymbol{T}$ is a disjoint union of disks $D \subset (\boldsymbol{T}, t)$ of one of the following three types:*

Type 0 *D separates the two strings of t.*

Type 1 *∂D decomposes as the union of two arcs $\alpha \cup \beta$ such that $\alpha \subset t$ and $\beta \subset \partial \boldsymbol{T}$.*

Type 2 *∂D decomposes as the union of four arcs $\alpha_1 \cup \beta_1 \cup \alpha_2 \cup \beta_2$ where $\alpha_i \subset t_i$ and $\beta_i \subset \partial \boldsymbol{T}$.*

Moreover, the isotopy decreases the number of bubbles that S meets and we may further assume that $\iota|_{\partial L} \colon \partial S \to L$ is a covering map.

Proof If no component of ∂S is a meridian, we may assume that up to isotopy $\iota|_{\partial L} \colon \partial S \to L$ is a covering map.

The twist box $(\boldsymbol{T}, t)$ is a trivial 2-tangle. The complement $\boldsymbol{T} \setminus \mathcal{N}(t)$ can be identified with $U \times [0,1]$, where U is a twice holed disk. Let E be the disk $\alpha \times [0,1]$, where α is the simple arc connecting the two holes of U. Up to a small isotopy, we may assume that S intersects E transversely. Since the bubbles in $\boldsymbol{T}$ are in some neighborhood of E, we may assume that S meets a bubble if it does so in E. The intersection $S \cap E$ comprises of simple closed curves and arcs. All curves and arcs except those connecting $\alpha \times \{0\}$ to $\alpha \times \{1\}$ can be eliminated by an isotopy pushing S off $\boldsymbol{T}$. This isotopy decreases the number of bubbles S meets. The number of bubbles the resulting surface meets equals the number of such arcs times the number of crossings in the corresponding twist region.

Up to isotopy, we may also assume that S intersects $U \times \{\frac{1}{2}\}$ transversely. Hence, $S \cap (U \times \{\frac{1}{2}\})$ is a collection of simple closed curves and arcs. By pushing S outwards towards the boundary of the disk U, one can assume that each component of $S \cap (U \times \{\frac{1}{2}\})$ is of the following form:

(0) An arc connecting the boundary of the disk U to itself separating the holes, and intersecting α once.

(1) An arc connecting a hole to the boundary of the disk and not intersecting α.

(2) An arc connecting the two holes and not intersecting α.

Thus, $S \cap (U \times [\frac{1}{2}-\varepsilon, \frac{1}{2}+\varepsilon])$ is a collection of disks of the form $\alpha \times [\frac{1}{2}-\varepsilon, \frac{1}{2}+\varepsilon]$, where α is an arc of type (0), (1) or (2) as stated. By an ambient isotopy, we can stretch the slab $U \times [\frac{1}{2}-\varepsilon, \frac{1}{2}+\varepsilon]$ to $U \times [0,1] = T$. The number of bubbles the resulting surface meets equals the number of arcs of type (0) times the number of twist in the twist region. The arcs of type (0) are in one-to-one correspondence with the arcs of $S \cap E$. Note that the fact that $\iota \colon \partial S \to L$ is a covering map was not affected by the isotopies above. □

Definition 3.2 A surface $S \subset \mathbb{S}^3 \setminus \mathcal{N}(L)$ is *in normal position* if it intersects the planes $P^{\pm}$ transversely and the map $\partial S \to L$ that is obtained by shrinking $\mathcal{N}(L)$ radially is a covering map onto its image. In particular, S has no meridional boundary components.

Lemma 3.3 *Let $S \subset \mathbb{S}^3 \setminus \mathcal{N}(L)$ be a surface in normal position, and let $(\boldsymbol{T}, t)$ be a twist box. Then, up to isotopy, each component of the intersection $S \cap \boldsymbol{T} \cap P^{\pm}$ looks as in Figure 3.* □

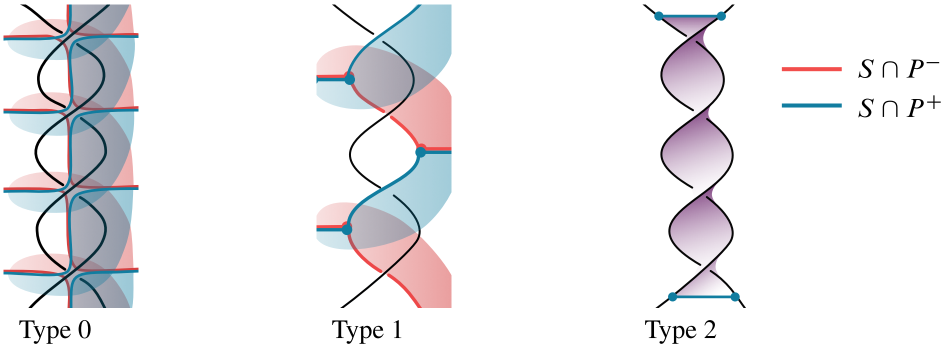

Figure 3: The possible three types of intersection of S with a twist box.

3.2 Curves of intersection

Let $S \subseteq \mathbb{S}^3 \smallsetminus \mathcal{N}(L)$ be a surface in normal position. We would like to study the surface S through its curves of intersection with the planes $P^{\pm}$.

Let $\mathcal{T}$ be the union of all twist boxes of L. Consider the collection of disks $\mathcal{D}$ of Type 2 which occur as intersections $S \cap \mathcal{T}$. We may assume that $\partial\mathcal{D} \subset P \cup L$, and that the subsurface $\widehat{S} = S \smallsetminus \mathcal{D}$ is transversal to $P^{\pm}$.

Recall the map $\iota\colon (S, \partial S) \to (\mathbb{S}^3, L)$. Define $\mathcal{C}^+ = \partial\iota^{-1}(\widehat{S} \cap H^+)$ and $\mathcal{C}^- = \partial\iota^{-1}(\widehat{S} \cap H^-)$. Now define $\mathcal{C} = \mathcal{C}^+ \cup \mathcal{C}^-$. As each of $P^{\pm}$ is a 2-sphere, $\widehat{S} \cap H^{\pm}$ is a collection of subsurfaces of $\widehat{S}$, the boundary of which are simple closed curves $c \subset S$. For $c \in \mathcal{C}^+$, denote by S_c the component of $\widehat{S} \cap H^+$ so that $c \subset \partial S_c$, and respectively for $c \in \mathcal{C}^-$.

We think of curves in $\mathcal{C}^{\pm}$ as curves on $P^{\pm}$, as they are disjoint outside L. Here, and in most of the figures in the remainder of this paper, curves in $\mathcal{C}^+$ are colored blue while curves in $\mathcal{C}^-$ are colored orange.

Assume S is in normal position, and let $\boldsymbol{T}$ be a twist box. The curves of intersection $\mathcal{C}$ of S which meet a connected component of $\iota(S) \cap \boldsymbol{T}$ must meet the corresponding twist region T in one of the following three configurations:

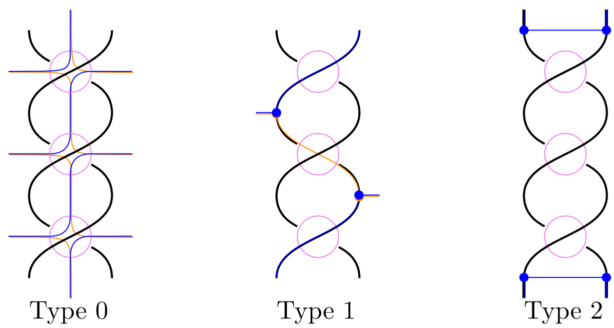

In order to analyze the curves $c \in \mathcal{C}$ we need to consider specific subarcs and points of c which we define next.

Definition 3.4 For a curve $c \in \mathcal{C}$, we define the following arcs and points (they are illustrated in the figures following the definition):

(1) An $\circ$-*joint* ("interior-joint") of c is a subarc of c which is a connected component of $c \cap \iota^{-1}(B)$ for some bubble B. The number of $\circ$-joints of c is denoted $\mathfrak{J}_\circ(c)$.

(2) A ∂-*joint* ("boundary-joint") of c is an endpoint of a connected component of $c \cap \partial S$. The number of ∂-joints of c is denoted $\mathfrak{J}_\partial(c)$

(3) A *joint* of c is an $\circ$-joint or a ∂-joint of c. The number of joints of c is denoted by $\mathfrak{J}(c) = \mathfrak{J}_\circ(c) + \mathfrak{J}_\partial(c)$.

(4) Define $\mathcal{C}_{i,j} = \{c \in \mathcal{C} \mid \mathfrak{J}_\circ(c) = i,\ \mathfrak{J}_\partial(c) = j\}$.

(5) A *bone* of c is a connected component of c minus its joints. Note that all bones are arcs which are mapped by ι to P.

(6) A ∂-*bone* of c is a bone which is contained in ∂S. Note that the endpoints of ∂-bones are ∂-joints. All other bones are $\circ$-*bones*.

(7) A *limb* of c is a subarc $\alpha \subset c$ with endpoints in the interiors of bones. Two limbs are equal if there is an isotopy of limbs (in c) between them. In particular, their endpoints lie in the interior of the same bones. The quantities $\mathfrak{J}(\alpha)$, $\mathfrak{J}_\circ(\alpha)$ and $\mathfrak{J}_\partial(\alpha)$ are defined as for curves.

(8) A *turn* of c is a limb of c that contains exactly one joint, this joint is an $\circ$-joint and the endpoints of the limb are outside twist regions. A curve *turns* at a twist region if it contains a turn in that region.

(9) A *wiggle* of c is a limb of c that contains exactly two joints, these joints are $\circ$-joints through consecutive bubbles of a twist box, and the endpoints of the limb are outside the twist regions. A curve *wiggles* through a twist region if it contains a wiggle in that region.

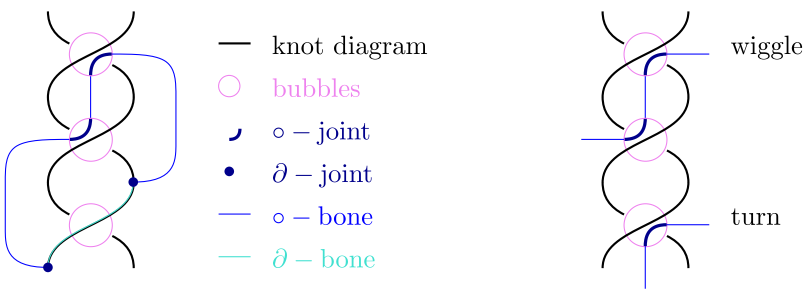

(10) Let $\mathcal{B}$ be a 3-ball bounded by a bubble B, then the components of $S \cap \mathcal{B}$ are *saddles*. Those are disks whose boundary is $\iota(\alpha_1^+ \cup \alpha_2^+ \cup \alpha_1^- \cup \alpha_2^-)$, where $\alpha_i^\pm$ are $\circ$-joints of curves in $\mathcal{C}^\pm$, respectively. The two $\circ$-joints α_1^+, α_2^+ (and the two $\circ$-joints α_1^-, α_2^-) are said to be *opposite*. See Figure 4.

Remark 3.5 Note that a ∂-joint connects a ∂-bone and $\circ$-bone, while a $\circ$-joint connects two $\circ$-bones. The ∂-joints and ∂-bones are contained in the boundary of S, while $\circ$-joints and $\circ$-bones are contained in the interior of S.

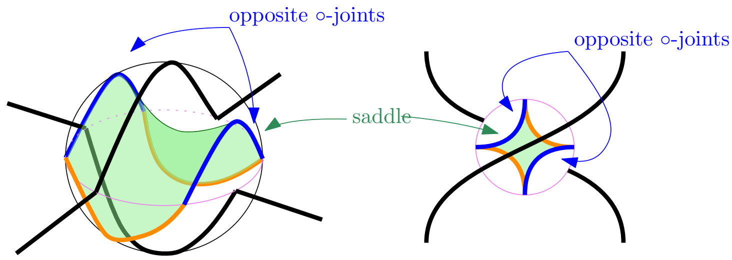

Figure 4: A saddle of S in a bubble viewed from an angle and from the top.

Definition 3.6 Two curves (or limbs of curves) $c, c' \in \mathcal{C}$ are *abutting* if they share an $\circ$-bone and $c \neq c'$. Necessarily, if $c \in \mathcal{C}^+$ then $c' \in \mathcal{C}^-$ and vice versa.

The following figure shows an example of two abutting curves c and c':

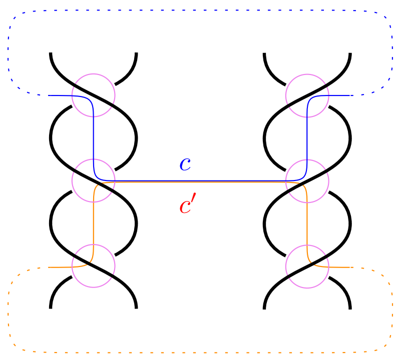

3.3 Taut surfaces

Definition 3.7 Given an incompressible surface $S \subset \mathbb{S}^3 \smallsetminus \mathcal{N}(L)$ we define a *lexicographic complexity* of S as

$$\mathrm{Com}(S) = \left(\sum_{c \in \mathcal{C}} \mathfrak{I}_\circ(c), \ \sum_{c \in \mathcal{C}} \mathfrak{I}_\partial(c), \ |\mathcal{C}| \right). \tag{3-1}$$

Recall that a properly embedded surface S in a 3-manifold M is called *essential* if it is either a 2-sphere which does not bound a 3-ball, or it is incompressible, boundary incompressible and not boundary parallel.

Definition 3.8 Let $S \subset \mathbb{S}^3 \smallsetminus \mathcal{N}(L)$ be an essential surface in normal position. The surface S is *taut* if either

(i) S is an essential 2-sphere, and S minimizes complexity among all essential 2-spheres, or

(ii) S is not a 2-sphere, the link L is not split (ie $\mathbb{S}^3 \smallsetminus L$ is irreducible), and S minimizes complexity in its isotopy class.

The next lemma shows that the intersection curves of taut surfaces must have certain properties.

Lemma 3.9 *Assume that the diagram $D(L)$ is connected. Let $S \subset \mathbb{S}^3 \smallsetminus \mathcal{N}(L)$ be a taut surface. Then, for all $c \in \mathcal{C}$ we have:*

(1) *S_c is a disk.*

(2) *$\mathfrak{J}_\partial(c)$ is even.*

(3) *If $\mathfrak{J}_\partial(c) \le 2$ then $\mathfrak{J}_\circ(c) > 0$.*

(4) *If $\mathfrak{J}_\partial(c) = 0$ then $\mathfrak{J}_\circ(c)$ is even.*

(5) *If a curve c meets a bubble B more than once, then it does so in two opposite $\circ$-joints.*

(6) *If a curve c has two ∂-joints on a connected component of $P^+ \cap L$ (or $P^- \cap L$), then they are the endpoints of a ∂-bone. Moreover, the two $\circ$-bones incident to them are in different regions of $P \smallsetminus D(L)$.*

(7) *The curve c is not a curve in $\mathcal{C}_{1,2}$ bounding on $P^\pm$ exactly one component of $L \cap P^\pm$ as depicted here:*

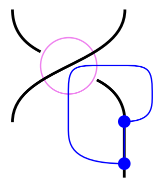

Proof Let $S \subset \mathbb{S}^3 \smallsetminus \mathcal{N}(L)$ be an essential surface satisfying (i) or (ii). Note that in both cases, compressing along a disk $D \subset \mathbb{S}^3 \smallsetminus \mathcal{N}(L)$ with $D \cap S = \partial D$ results either in two essential spheres, or a surface in the same isotopy class of S. Thus, by the assumption on S, surfaces obtained by such a compression cannot have lower complexity.

(1) Since S is essential, each subsurface S_c must be planar, as otherwise it contains a nontrivial compression disk. If S_c has more than one boundary component then compressing along a disk in H^+ or H^- whose boundary separates boundary components of S_c will result in a surface with fewer intersections with P in contradiction to the choice of S.

(2) By definition, $\mathfrak{J}_\partial(c)$ is the number of endpoints of arcs in $c \smallsetminus L$. Since each arc has two endpoints, $\mathfrak{J}_\partial(c)$ is even.

(3) By (2), $\mathfrak{J}_\partial(c)$ is either two or zero. If $\mathfrak{J}_\partial(c) = 0$ and $\mathfrak{J}_\circ(c) = 0$ then, since $D(L)$ is connected, c bounds a disk on $P \smallsetminus L$. Compressing S along this disk reduces the number of intersections with P.

If $\mathfrak{J}_\partial(c) = 2$ and $\mathfrak{J}_\circ(c) = 0$ then c bounds a disk D in P such that $\partial D = \alpha \cup \beta$, where α is a ∂-bone of c and β is an $\circ$-bone of c. However, this is impossible by (2).

(4) The diagram $D(L)$ is a 4-regular graph, and thus it partitions P into regions which can be given a checkerboard coloring, ie can be colored black and white so that two adjacent regions are colored in different colors. Consider the colors of complementary regions of $P \smallsetminus \mathcal{T}$ which the curve c intersects. If $\mathfrak{J}_\partial(c) = 0$ every change of colors, of these regions along c, accounts for one bubble that c meets. Since c is a closed curve the total number of color changes is even, and correspondingly $\mathfrak{J}_\circ(c)$ is even.

(5) Without loss of generality assume that $c \in \mathcal{C}^+$. Each time c meets a bubble B it does so along a ∂-bone or an $\circ$-joint. Since c meets B twice then it does so along either two ∂-bones, an $\circ$-joint and a ∂-bone or two $\circ$-joints. If c meets B in two ∂-bones, then the disk S_c contains an arc connecting the two ∂-bones. This arc together with an arc on $\partial\mathcal{N}(L)$ bounds (by an innermost argument) a compression disk for S. Compressing along this disk reduces the complexity of S.

If c meets B in an $\circ$-joint and a ∂-bone, then the disk S_c contains an arc connecting the $\circ$-joint and the ∂-bone. This arc, together with an arc on B bounds a disk. Isotoping S through this disk reduces the complexity of S.

Thus, c meets B in two $\circ$-joints. Assume that c has two $\circ$-joints in B on the same side of L as in

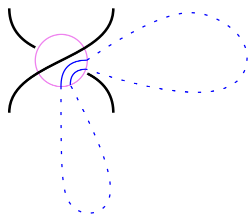

The isotopy of S defined in the proof of Lemma 1(ii) of [11] (for the case $R \cap L = \varnothing$ in his notation) reduces our complexity since the number $\sum_{c \in \mathcal{C}} \mathfrak{J}_\circ(c)$ strictly decreases.

By Lemma 1(ii) of [11], c does not have It follows that c has at most two $\circ$-joints in the same bubble, and they are separated by L in B^+. The number of components of $S \cap B^+$ separating each of the $\circ$-joints of c from L is the same: Each component of $S \cap B$ separating an $\circ$-joint of c and L belongs to a curve c' in $\mathcal{C}^+$. As curves in $\mathcal{C}^+$ do not intersect, in order to close up, c' has to return to B on the other side of L between L and the other $\circ$-joint of c in B. This is depicted here:

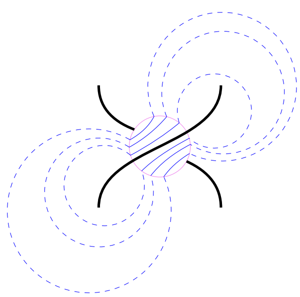

The intersection of S with the ball bounded by B, is a finite collection of stacked saddles, it follows that the $\circ$-joints of c belong to the same saddle.

(6) If c has two ∂-joints on the same component of $P^+ \cap L$. Let α in $P^+ \cap L$ and β in S_c be arcs connecting the two ∂-joints. Unless α is a ∂-bone of c, by compressing along the disk bounded by $\alpha \cup \beta$ (using an innermost such disk) complexity is reduced because $\sum_{c \in \mathcal{C}} \mathfrak{J}_\partial(c)$ strictly decreases while $\sum_{c \in \mathcal{C}} \mathfrak{J}_\circ(c)$ does not increase.

If c contains a ∂-bone α such that the two adjacent $\circ$-joints are in the same region of $P \smallsetminus D(L)$ then, by pushing S through P in a neighborhood of α, we reduce the number of intersection points by 2, in contradiction to the minimal complexity of S.

(7) Assume in contradiction that c is such a curve, ie as the blue curve here:

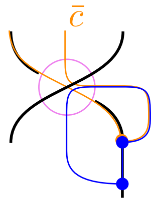

By (6), any curve contained in c has to be of a similar form. Assume c is an innermost such curve. The curve $\bar{c}$ abutting c, as depicted in the following figure, meets the bubble twice, at a ∂-bone and an $\circ$-joint, in contradiction to (5). □

Remark 3.10 Note that if S is taut then $\mathcal{C}_{0,0} = \mathcal{C}_{0,2} = \mathcal{C}_{i,2k+1} = \mathcal{C}_{2k+1,0} = \varnothing$ for all $i, k \in \mathbb{N} \cup \{0\}$.

4 Euler characteristic and curves of intersection

From now on we assume that the surface S is taut.

4.1 Distributing Euler characteristic among curves

For each curve $c \in \mathcal{C}$ we will define the *contribution* of c, and show that the Euler characteristic of S can be computed by summing up the contributions of curves $c \in \mathcal{C}$.

Definition 4.1 The *contribution* $\chi_+(c)$ of a curve $c \in \mathcal{C}$ is defined by

$$\chi_+(c) = 1 - \tfrac{1}{4}\mathfrak{J}(c).$$

Lemma 4.2 *If $S \subset \mathbb{S}^3 \smallsetminus \mathcal{N}(L)$ is taut then $\chi(S) = \sum_{c \in \mathcal{C}} \chi_+(c)$.*

Proof The union of the collection of all the curves $c \in \mathcal{C}$ on S is an embedded graph $\widehat{X}$ of S. The vertices $\widehat{X}^0$ of the graph $\widehat{X}$ are the ∂-joints and the endpoints of $\circ$-joints. The edges $\widehat{X}^1$ of the graph $\widehat{X}$ are the bones and the $\circ$-joints. The graph $\widehat{X}$ partitions S into disk regions of three types:

1. subsurfaces $S_c \subseteq \widehat{S} \cap H^{\pm}$ for $c \in \mathcal{C}^{\pm}$,
2. saddles $R \subseteq \widehat{S} \cap \mathcal{B}$ where $\mathcal{B}$ is a 3-ball bounded by a bubble, or
3. regions $D \subset S$ corresponding to Type 2 disks.

In case (3), the regions D are disks whose boundary consists of two arcs on L and two edges of $\widehat{X}$. By collapsing each such disk D to one of the edges in $\widehat{X}$ we get a homotopic surface. By abuse of notation, we call it S, and call the corresponding graph X obtained from $\widehat{X}$ by gluing together pairs of $\circ$-bones. Note that in the new surface, $\partial S \subset X$ and consists of circles comprised of ∂-bones and ∂-joints. Moreover, along every $\circ$-bone there are two abutting curves. It follows that

$$\chi(S) = \chi(X) + \sum_{S' \subseteq \widehat{S} \cap H^{\pm}} \chi(S') + \sum_{R \subseteq \widehat{S} \cap B} \chi(R) = |X^0| - |X^1| + \sum_{S' \subseteq \widehat{S} \cap H^{\pm}} \chi(S') + \sum_{R \subseteq \widehat{S} \cap B} \chi(R). \tag{4-1}$$

We compute how each $c \in \mathcal{C}$ contributes to each of the summands in (4-1):

The vertices of X Every curve $c \in \mathcal{C}$ passes through $2\mathfrak{J}_\circ(c)$ vertices of X^0 in the interior of S (those are the endpoints of $\circ$-joints it passes). Furthermore, it goes through $\mathfrak{J}_\partial(c)$ vertices of X^0 in ∂S. Each of these vertices belongs to two (abutting) curves $c \in \mathcal{C}$. Hence,

$$|X^0| = \sum_{c \in \mathcal{C}} \big(\mathfrak{J}_\circ(c) + \tfrac{1}{2}\mathfrak{J}_\partial(c)\big) \tag{4-2}$$

The edges of X Every curve $c \in \mathcal{C}$ passes through $2\mathfrak{J}_\circ(c) + \mathfrak{J}_\partial(c)$ edges in X^1. Note that every $\circ$-joint edge and every ∂-bone edge belongs to exactly one curve in $\mathcal{C}$, while each $\circ$-bone edge belongs to two curves in $\mathcal{C}$. Each $\circ$-joint edge appears in exactly one curve c and is counted once in $\mathfrak{J}_\circ(c)$. Hence, the number of $\circ$-joint edges is $\sum_{c \in \mathcal{C}} \mathfrak{J}_\circ(c)$. Similarly each ∂-bone edge appears in exactly one curve c and is counted twice in $\mathfrak{J}_\partial(c)$. Hence, the number of ∂-bone edges is $\sum_{c \in \mathcal{C}} \frac{1}{2}\mathfrak{J}_\partial(c)$. Finally, each $\circ$-bone edge in c accounts for two vertices in X^0. So the number of $\circ$-bone edges is equal to

$$\tfrac{1}{2}|X^0| = \tfrac{1}{2}\Big(\sum_{c \in \mathcal{C}} \big(\mathfrak{J}_\circ(c) + \tfrac{1}{2}\mathfrak{J}_\partial(c)\big)\Big).$$

Adding these contributions together gives

$$|X^1| = \sum_{c \in \mathcal{C}} \big(\tfrac{3}{2}\mathfrak{J}_\circ(c) + \tfrac{3}{4}\mathfrak{J}_\partial(c)\big). \tag{4-3}$$

Regions $S' \subset \widehat{S} \cap H^{\pm}$ To every curve $c \in \mathcal{C}$ there is a disk $S_c \subseteq \widehat{S} \cap H^{\pm}$. Thus,

$$\sum_{S' \subseteq \widehat{S} \cap H^{\pm}} \chi(S') = \sum_{c \in \mathcal{C}} 1. \tag{4-4}$$

Saddle regions $R \subset \widehat{S} \cap \mathcal{B}$ Each $\circ$-joint of a curve $c \in \mathcal{C}$ belongs to the boundary such a region. And so each curve passes through the boundary of $\mathfrak{J}_\circ(c)$ such regions. As each saddle region has four $\circ$-joints in its boundary, we have

$$\sum_{R \subseteq \widehat{S} \cap B} \chi(R) = \sum_{c \in \mathcal{C}} \tfrac{1}{4}\mathfrak{J}_\circ(c). \tag{4-5}$$

Summing over all of the above we get,

$$\begin{aligned}\chi(S) &= |X^0| - |X^1| + \sum_{S' \subseteq \widehat{S} \cap H^{\pm}} \chi(S') + \sum_{R \subseteq \widehat{S} \cap B} \chi(R) \\ &= \sum_{c \in \mathcal{C}} \left(1 - \tfrac{1}{4}(\mathfrak{I}_{\circ}(c) + \mathfrak{I}_{\partial}(c))\right) \\ &= \sum_{c \in \mathcal{C}} \chi_{+}(c). \qquad \square\end{aligned}$$

5 Redistribution of Euler characteristic

Standing assumption Throughout the rest of the paper, we assume that the diagram $D(L)$ is connected, prime, twist-reduced, 3-highly twisted and contains at least two twist regions.

In this section we redistribute the positive contribution of the Euler characteristic of curves, χ_{+}, so that after the redistribution each curve's contribution is nonpositive.

We first characterize the curves of intersection that have a positive χ_{+}. The characterization is done in the following lemma:

Lemma 5.1 *Let $c \in \mathcal{C}$ so that $\chi_{+}(c) > 0$ (ie $\mathfrak{I}(c) < 4$) then $c \in \mathcal{C}_{2,0}$ or $c \in \mathcal{C}_{1,2}$ and it is one of the six forms of Figure 5 (up to isotopy).*

Note that the curves c in cases (i) and (ii) are in $\mathcal{C}_{2,0}$. The curves in cases (iii), (iv), (v) and (vi) belong to $\mathcal{C}_{1,2}$.

Proof It follows from Definition 4.1, Lemma 3.9 and Remark 3.10 that if $\chi_{+}(c) > 0$ then $c \in \mathcal{C}_{2,0}$ or $c \in \mathcal{C}_{1,2}$. Since the diagram is prime, a curve $c \in \mathcal{C}_{2,0}$ must contain two turns at different twist boxes. Hence c is as depicted in figures (i) or (ii).

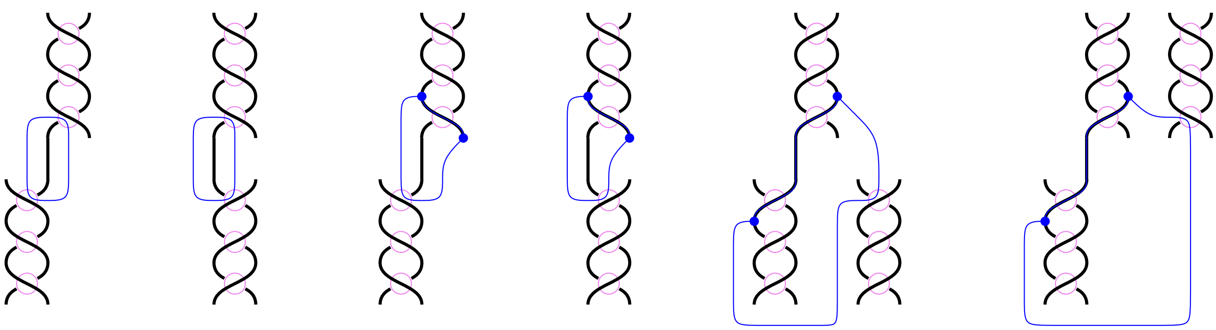

(i) (ii) (iii) (iv) (v) (vi)

Figure 5: The six possibilities for a curve in $c \in \mathcal{C}_{2,0} \cup \mathcal{C}_{1,2}$.

Let $c \in \mathcal{C}_{1,2}$ and let α denote a limb which is a small extension of the unique ∂-bone in c. The endpoints of α must be in regions of $P \smallsetminus D(L)$ of different color since the complementary limb of α in c is a turn. Since S is taut, Lemma 3.9(7) implies that α must pass over at least one crossing of $D(L)$. Since the endpoints of α are in regions of different colors, α cannot connect the two regions adjacent to the two length edges of a twist region. Thus, α enters a twist region T through its length edge, and exists on L. It can meet one or two twist regions. If α meets one twist region, then it must be as in figures (iii) or (iv). Otherwise, up to isotopy, it must be as in figures (v) or (vi). □

Definition 5.2 Denote by $\mathcal{C}_{>0}$ (resp. $\mathcal{C}_{\leq 0}$) the set of curves $c \in \mathcal{C}$ such that $\chi_+(c) > 0$ (resp. ≤ 0). The lemma above shows that $\mathcal{C}_{>0} = \mathcal{C}_{2,0} \cup \mathcal{C}_{1,2}$. The *type* of a curve in $\mathcal{C}_{>0}$ corresponds to the types of curves as depicted in Figure 5. For example, a curve of $\mathcal{C}_{2,0}$ is of type (i) or (ii).

Next, we will describe a distinguished set, denoted by $\mathcal{K}$, of limbs of curves in $\mathcal{C}$ to which we will "reallocate" some of the positive contribution of curves in $\mathcal{C}_{>0}$. We begin with a definition:

Definition 5.3 An *extremal* bubble is a first or last bubble of a twist region. A curve wiggles *extremally* if it wiggles through an extremal bubble. Assume that a curve or an arc β wiggles through a twist region extremally, then the $\circ$-bone $\alpha \subset \beta$ which leaves the twist region from the extremal bubble of the wiggle is called a *core* of β.

Definition 5.4 A *vertebra* is an $\circ$-bone τ in a curve c connecting two turns of c in two twist regions T, T' so that τ meets the length edge of T and the width edge of T'.

A *rib* is a closed curve $c \in \mathcal{C}_{4,0}$ which consists of exactly two turns and an extremal wiggle.

Remark 5.5 Note that the two $\circ$-bones of a curve $c \in \mathcal{C}_{2,0}$ of type (i) are vertebrae.

Lemma 5.6 *Assume that c_0 is not a rib, and that c_0 contains a vertebra τ_0. Then, there exists a finite sequence of curves $c_0, c_1, \dots, c_n$, limbs $\kappa_1, \dots, \kappa_n$ and bones $\tau_0, \dots, \tau_{n-1}$ such that:*

(1) *For $1 \leq i < n$, c_i is a rib and τ_i is the $\circ$-bone connecting its two turns.*
(2) *For $1 \leq i \leq n$, κ_i is a limb of c_i with a unique core τ_{i-1} and $\mathfrak{J}(\kappa_i) = 3$. In particular, the curve c_i abuts the curve c_{i-1} along the core τ_{i-1}.*
(3) *The curve c_n has $\chi_+(c_n) < 0$.*

Moreover, given κ_n one can uniquely determine the $\circ$-bone τ_0 and hence the curves c_i, arcs κ_i and bones τ_i as above.

Definition 5.7 We will refer to the curves c_i (resp. limbs κ_i) in the lemma as the *layers curves* (resp. *layer limbs*) of τ_0, and to the curve c_n (resp. arc κ_n) as the *terminal layer curve* (resp. *terminal layer limb*) of τ_0.

Proof of Lemma 5.6 We produce a sequence of curves, limbs and bones, satisfying the assumptions above, which terminates at the first curve c_n such that $\chi_+(c_n) < 0$.

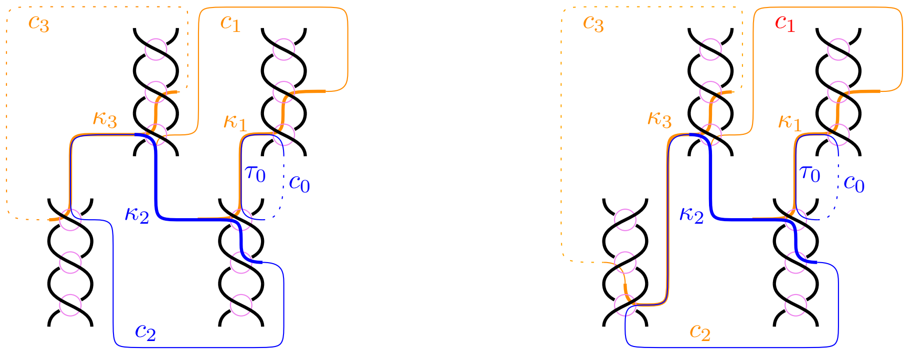

Figure 6: Example 5.8.

Let c_0 and τ_0 be as in the statement of the lemma. Let c_1 be the curve abutting c_0 along τ_0. The bone τ_0 connects an extremal wiggle and a turn of c_1, hence it is a core of c_1. Let κ_1 be the limb of c_1 containing τ_0 and the adjacent wiggle and turn. If $\chi_+(c_1) < 0$, then stop the process. Otherwise, $\mathfrak{J}(c_1) = 4$. Hence, by Lemma 3.9, the curve c_1 is a rib, ie it consists of a wiggle and two turns and has a unique core. Let α_1, α_1' be the $\circ$-joint of the two turns of c_1, and assume that $\alpha_1 \subset \kappa_1$. Let τ_1 be the $\circ$-bone of c_1 connecting α_1, α_1'. The bone τ_1 meets the length edge of the twist region containing α_1.

Assume first that τ_1 is not a vertebra of c_1, ie it meets the length edge of the twist region containing α_1'. Then, the curve c_2 abutting c_1 along τ_1 contains two wiggles in two different twist regions. It follows that $\chi_+(c_2) < 0$ as otherwise c_2 bounds a twist reduction subdiagram. Let κ_2 be the limb in c_2, abutting τ_1, consisting of a wiggle through the bubble of α_1, and one more $\circ$-joint at the bubble containing α_1'. The bone τ_1 is the unique core of the limb κ_2, and the process stops ($n = 2$).

If τ_1 is a vertebra, then we iterate the process. That is, we consider the curve c_2 abutting c_1 along τ_1, and the limb κ_2 of c_2 containing τ_1 and its adjacent wiggle and turn.

Since there are finitely many curves and limbs, the process either terminates or is periodic. It cannot be periodic because the initial curve c_0 is not a rib, but note that all the curves c_i for $i < n$ are ribs.

Finally, given κ_n, the curve c_{n-1} is the curve abutting c_n along the unique core of κ_n. The curve c_{n-1} has a unique core, which is also the core of a unique arc κ_{n-1} (with $\mathfrak{J}(\kappa_{n-1}) = 3$). Repeating this process, we can retrace the sequence all the way to τ_0. □

Example 5.8 In Figure 6 we see two examples of outputs of the process in Lemma 5.6. Starting with the curve c_0 which is not a rib, and the vertebra τ_0 of c_0, we get the curves c_0, c_1, c_2, c_3, limbs $\kappa_1, \kappa_2, \kappa_3$ and $\circ$-bones τ_0, τ_1, τ_2. The limbs κ_i are shown in bold the figure. The $\circ$-bones τ_0, τ_1, τ_2 are the cores of $\kappa_1, \kappa_2, \kappa_3$ respectively.

In Figure 6, left, note that the $\circ$-bone τ_2 is a vertebra. If $\chi_+(c_3) < 0$ then the process stops at c_3 and κ_3 is its terminal limb. Otherwise, c_3 is again a rib, and the process continues.

In Figure 6, right, the $\circ$-bone connecting the two turns of c_2 is not a vertebra, as it meets the length edge of both twist regions. Therefore the limb κ_3, which is shown in bold in the figure, contains a wiggle (through the bubble in which both c_1 and c_2 turn) and "half a wiggle" (through the other bubble in which c_2 turns). As the proof shows, the curve c_3 necessarily satisfies $\chi_+(c_3) < 0$, and thus it is the terminal curve of the process.

Definition 5.9 (definition of $\mathcal{K}$) (1) Each $c \in \mathcal{C}_{2,0}$ of type (i) has two $\circ$-bones. Each $\circ$-bone τ of c is a vertebra and hence by Lemma 5.6 determines a terminal layer limb κ_n. Let $\mathcal{K}_{3,0}$ be the set of all terminal layer limbs associated with all $\circ$-bones of curves in $c \in \mathcal{C}_{2,0}$.

(2) Each $c \in \mathcal{C}_{2,0}$ of type (ii) determines an arc κ which abuts c and wiggles through the two twist regions. Let $\mathcal{K}_{4,0}$ be the collection of all arcs κ obtained in this way.

(3) Each $c \in \mathcal{C}_{2,1}$, determines an arc κ which abuts c, wiggles through the twist region in which c turns, and contains one of the ∂-joints of c. Let $\mathcal{K}_{2,1}$ be the collection of all arcs κ obtained in this way.

Finally, let $\mathcal{K}$ be the set $\mathcal{K}_{3,0} \cup \mathcal{K}_{4,0} \cup \mathcal{K}_{2,1}$.

Lemma 5.10 *Given $\kappa \in \mathcal{K}$ one can uniquely determine the curve $c \in \mathcal{C}_{>0}$ that determines it. Conversely, to each curve in $\mathcal{C}_{2,0}$ of type* (i) *there are two curves of $\mathcal{K}_{3,0}$ corresponding to the two choices of $\circ$-bones of c. To each curve in $\mathcal{C}_{1,2}$ and each curve in $\mathcal{C}_{2,0}$ of type* (ii) *there is a unique arc in $\mathcal{K}_{2,1}$ and $\mathcal{K}_{4,0}$ respectively.*

In particular,
$$\tfrac{1}{2}|\mathcal{K}_{3,0}| + |\mathcal{K}_{4,0}| = |\mathcal{C}_{2,0}| \quad \textit{and} \quad |\mathcal{K}_{2,1}| = |\mathcal{C}_{1,2}|.$$

Proof If $\kappa \in \mathcal{K}_{4,0}$ (resp. $\kappa \in \mathcal{K}_{2,1}$) then the curve $c \in \mathcal{C}_{2,0}$ of type (ii) (resp. $c \in \mathcal{C}_{1,2}$) that determines it is the curve abutting κ. If $\kappa \in \mathcal{K}_{3,0}$ then by Lemma 5.6 there is a unique $\circ$-bone τ of a curve $\mathcal{C}_{2,0}$ of type (i) that determines it. The converse statements follow. □

Lemma 5.11 *The arcs in $\mathcal{K}$ which belong to curves in $\mathcal{C}^+$ (resp. $\mathcal{C}^-$) are pairwise disjoint.*

Proof Assume that the two arcs $\kappa, \kappa' \in \mathcal{K}$ meet. Since, by Lemma 5.10, every arc in $\mathcal{K}$ is determined by its core, it suffices to show that κ and κ' have the same core.

By assumption κ, κ' share a joint, and hence are limbs of the same curve c. If this joint is a ∂-joint then $\kappa, \kappa' \in \mathcal{K}_{2,1}$ and their core is the unique $\circ$-bone incident to their shared ∂-joint. If the joint is an $\circ$-joint that is part of a wiggle of c, then, since the diagram is 3-highly twisted, there is a unique core emanating from the extremal bubble of this wiggle, which is shared by both κ and κ'. Finally, if the joint is an $\circ$-joint that is part of a turn of c, then $\kappa, \kappa' \in \mathcal{K}_{3,0}$. The cores of κ, κ' must be the unique $\circ$-bone which emanates from the width edge of the twist region in which the turn occurs because it is also the vertebra of the previous layer curve. □

Lemma 5.12 *For all $\kappa \in \mathcal{K}$ we have $\mathfrak{J}(c) \geq \mathfrak{J}(\kappa) + 2$, where c is the unique curve in $\mathcal{C}$ containing κ.*

Proof Let $\kappa \in \mathcal{K}$ and let $c \in \mathcal{C}$ be the curve containing κ. Assume for contradiction that $\mathfrak{J}(c) < \mathfrak{J}(\kappa) + 2$.

If $\kappa \in \mathcal{K}_{4,0}$ then $\mathfrak{J}(c) < \mathfrak{J}(\kappa) + 2$ implies that $c \in \mathcal{C}_{4,0}$. If this is the case, then since c wiggles through two twist regions, the projection of c to P gives a twist-reduction subdiagram in contradiction to the assumption on the diagram.

If $\kappa \in \mathcal{K}_{2,1}$, then $\mathfrak{J}(c) < \mathfrak{J}(\kappa) + 2$ implies that $c \in \mathcal{C}_{2,2}$. If this is the case, then κ abuts some curve $c_0 \in \mathcal{C}_{1,2}$ which could be one of the figures (iii)–(vi) in Lemma 5.1. For case (iii), there are two possible configurations for the closed curve $c \in \mathcal{C}_{2,2}$ containing κ, while for each of the cases (iv)–(vi) there is only one possible such curve. Thus, all possible cases for the curve c are shown here:

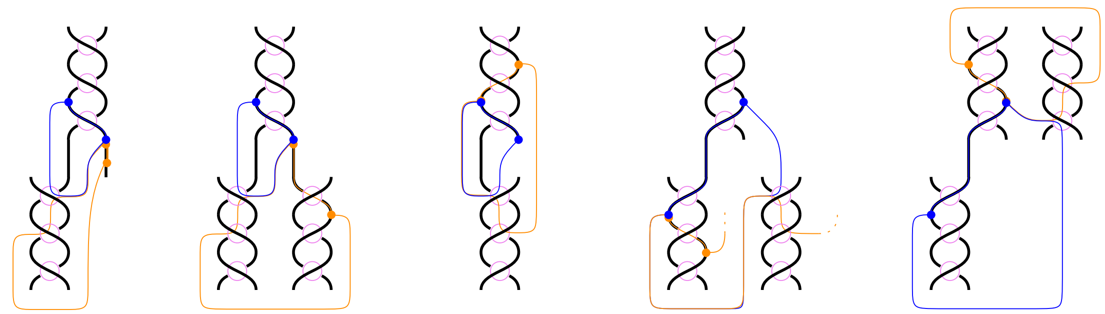

(iii) (iii′) (iv) (v) (vi)

In case (iii) the surface is not taut and in all other cases, the curve c bounds a twist-reduction subdiagram.

If $\kappa \in \mathcal{K}_{3,0}$, then $\mathfrak{J}(c) < \mathfrak{J}(\kappa) + 2$ implies that $c \in \mathcal{C}_{4,0}$, however this is in contradiction to the definition of $\mathcal{K}_{3,0}$ given by Lemma 5.6. □

Remark 5.13 It follows from the proof of Lemma 5.6 that if c contains a limb $\kappa \in \mathcal{K}_{3,0}$ such that the core of τ is not a vertebra of its abutting curve then $\mathfrak{J}(c) \geq \mathfrak{J}(k) + 3$: Indeed, if $c = c_n$, $\kappa = \kappa_n$ and κ abuts c_{n-1} along a bone which is not a vertebra of c_{n-1} then c must have an additional $\circ$-joint which is not contained in κ.

Definition 5.14 Let $c \in \mathcal{C}$. If $c \in \mathcal{C}_{>0}$ define $\chi'(c) = 0$. Otherwise, let $n_{3,0}$ (resp. $n_{4,0}$; $n_{2,1}$) be the number of limbs $\kappa \in \mathcal{K}_{3,0}$ (resp. $\mathcal{K}_{4,0}$; $\mathcal{K}_{2,1}$) in c. We associate to c the quantity

$$\chi'(c) = \chi_+(c) + \tfrac{1}{4}n_{3,0} + \tfrac{1}{2}n_{4,0} + \tfrac{1}{4}n_{2,1}.$$

The next lemma shows that χ' is a redistribution of the Euler characteristic of S among curves in $\mathcal{C}_{\leq 0}$.

Lemma 5.15

$$\chi(S) = \sum_{c \in \mathcal{C}} \chi'(c).$$

Proof By Lemma 4.2, $\chi(S) = \sum_{c \in \mathcal{C}} \chi_+(c)$. Since $\chi'(c) = 0$ for $c \in \mathcal{C}_{>0}$,

$$\sum_{c \in \mathcal{C}} \chi'(c) = \sum_{c \in \mathcal{C}_{\leq 0}} \chi'(c).$$

It thus remains to prove that

$$\sum_{c\in\mathcal{C}}\chi_+(c)=\sum_{c\in\mathcal{C}_{\le 0}}\chi'(c).$$

Subtracting $\sum_{c\in\mathcal{C}_{\le 0}}\chi_+(c)$ from both sides and recalling that $\mathcal{C}_{\le 0}=\mathcal{C}\smallsetminus\mathcal{C}_{>0}$, we have to show that

$$\sum_{c\in\mathcal{C}_{>0}}\chi_+(c)=\sum_{c'\in\mathcal{C}_{\le 0}}(\chi'(c')-\chi_+(c')).$$

The left hand side is simply $\frac{1}{2}|\mathcal{C}_{2,0}|+\frac{1}{4}|\mathcal{C}_{1,2}|$ since $\mathcal{C}_{>0}=\mathcal{C}_{2,0}\cup\mathcal{C}_{1,2}$ and

$$\chi_+(c)=\begin{cases}\frac{1}{2} & \text{if } c\in\mathcal{C}_{2,0},\\ \frac{1}{4} & \text{if } c\in\mathcal{C}_{1,2}.\end{cases}$$

By the definition of χ', the right hand side gives $\frac{1}{4}|\mathcal{K}_{3,0}|+\frac{1}{2}|\mathcal{K}_{4,0}|+\frac{1}{4}|\mathcal{K}_{2,1}|$. The proof is now complete by Lemma 5.10. □

The next lemma shows that indeed χ' is nonpositive.

Lemma 5.16 $\chi'(c)\le 0$ *for all* $c\in\mathcal{C}$.

Proof If $c\in\mathcal{C}_{>0}$ then $\chi'(c)=0$. Let $c\in\mathcal{C}_{\le 0}$ and let $n_{3,0},n_{4,0},n_{2,1}$ be as in Definition 5.14 of $\chi'(c)$. By Lemma 5.11, the limbs of $\mathcal{K}$ in c are disjoint and therefore

$$\mathfrak{I}(c)\ge\sum_{c\supset\kappa\in\mathcal{K}}\mathfrak{I}(\kappa). \tag{5-1}$$

Hence,

$$\begin{aligned}\chi'(c)&=\chi_+(c)+\tfrac{1}{4}n_{3,0}+\tfrac{1}{2}n_{4,0}+\tfrac{1}{4}n_{2,1}=\bigl(1-\tfrac{1}{4}\mathfrak{I}(c)\bigr)+\tfrac{1}{4}n_{3,0}+\tfrac{1}{2}n_{4,0}+\tfrac{1}{4}n_{2,1}\\ &\le 1-\sum_{c\supset\kappa\in\mathcal{K}}\tfrac{1}{4}\mathfrak{I}(\kappa)+\tfrac{1}{4}n_{3,0}+\tfrac{1}{2}n_{4,0}+\tfrac{1}{4}n_{2,1}\\ &=1+\sum_{c\supset\kappa\in\mathcal{K}_{3,0}}\bigl(\tfrac{1}{4}-\tfrac{1}{4}\mathfrak{I}(\kappa)\bigr)+\sum_{c\supset\kappa\in\mathcal{K}_{4,0}}\bigl(\tfrac{1}{2}-\tfrac{1}{4}\mathfrak{I}(\kappa)\bigr)+\sum_{c\supset\kappa\in\mathcal{K}_{2,1}}\bigl(\tfrac{1}{4}-\tfrac{1}{4}\mathfrak{I}(\kappa)\bigr)\\ &=1+\sum_{c\supset\kappa\in\mathcal{K}_{3,0}}\bigl(\tfrac{1}{4}-\tfrac{1}{4}\cdot 3\bigr)+\sum_{c\supset\kappa\in\mathcal{K}_{4,0}}\bigl(\tfrac{1}{2}-\tfrac{1}{4}\cdot 4\bigr)+\sum_{c\supset\kappa\in\mathcal{K}_{2,1}}\bigl(\tfrac{1}{4}-\tfrac{1}{4}\cdot 3\bigr)\\ &=1-\tfrac{1}{2}(n_{3,0}+n_{4,0}+n_{2,1}).\end{aligned} \tag{5-2}$$

Now the argument is divided into cases depending on the sum $n=n_{3,0}+n_{4,0}+n_{2,1}$.

Case 0 ($n=0$) We have $\chi'(c)=\chi_+(c)$. But since $c\in\mathcal{C}_{\le 0}$ we have $\chi_+(c)\le 0$ and we are done.

Case 1 ($n=1$) That is, c contains a single subarc $\kappa\in\mathcal{K}_{3,0}\cup\mathcal{K}_{4,0}\cup\mathcal{K}_{2,1}$. By Lemma 5.12, $\mathfrak{I}(c)\ge\mathfrak{I}(\kappa)+2$. If $\kappa\in\mathcal{K}_{4,0}$ we get $\mathfrak{I}(c)\ge 6$ and thus $\chi'(c)=1-\frac{1}{4}\mathfrak{I}(c)+\frac{1}{2}\le 0$. Similarly, if $\kappa\in\mathcal{K}_{3,0}\cup\mathcal{K}_{2,1}$ we get $\mathfrak{I}(c)\ge 5$ and thus $\chi'(c)=1-\frac{1}{4}\mathfrak{I}(c)+\frac{1}{4}\le 0$.

Case 2 ($n\ge 2$) In this case we are done by inequality (5-2). □

Corollary 5.17 *The link* $\mathcal{L}$ *is nonsplit nor the unknot.*

name of set	$\mathfrak{J}(\cdot)$	$\mathfrak{J}_\circ(\cdot)$	$\mathfrak{J}_\partial(\cdot)$	the set's composition/classification
$\mathcal{C}_{2,0}$	2	2	0	type (i) or (ii)
$\mathcal{C}_{1,2}$	3	1	2	type (iii), (iv) or (v)
$\mathcal{C}_{4,0}$	4	4	0	4 turns or 1 wiggle and 2 turns or 2 wiggles
$\mathcal{C}_{2,2}$	4	2	2	2 $\circ$-joints and 1 ∂-bone
$\mathcal{C}_{0,4}$	4	0	4	2 ∂-bones
$\mathcal{K}_{3,0}+0,2$	5	3	2	1 limb of $\mathcal{K}_{0,3}$ + ∂-bone
$\mathcal{K}_{2,1}+1,1$	5	3	2	1 limb of $\mathcal{K}_{2,1}$ + 1 $\circ$-joint + 1 ∂-joint
$\mathcal{K}_{4,0}+2,0$	6	6	0	1 limb of $\mathcal{K}_{0,4}$ + 2 $\circ$-joints
$\mathcal{K}_{4,0}+0,2$	6	4	2	1 limb of $\mathcal{K}_{0,4}$ + ∂-bone
$\mathcal{K}_{3,0}+\mathcal{K}_{3,0}$	6	6	0	2 limbs of $\mathcal{K}_{3,0}$ = 2 wiggles + 2 turns
$\mathcal{K}_{2,1}+\mathcal{K}_{2,1}$	6	4	2	2 limbs of $\mathcal{K}_{2,1}$ = 2 wiggles + ∂-bone
$\mathcal{K}_{4,0}+\mathcal{K}_{4,0}$	8	8	0	2 limbs of $\mathcal{K}_{4,0}$ = 4 wiggles

Table 1: Classification of all curves with $\chi'(c)=0$.

Proof Assume, in contradiction, that $\mathbb{S}^3 \smallsetminus \mathcal{N}(\mathcal{L})$ has an essential sphere or a disk bounding a component of L. By Lemma 3.9 we may assume that S is taut. Let $\mathcal{C}$ be its curves of intersection With $P^{\pm}$. By Lemma 5.15,

$$0<\chi(S)=\sum_{c\in\mathcal{C}}\chi'(c).$$

However, this contradicts Lemma 5.16 which states that $\chi'(c)\le 0$ for all $c\in\mathcal{C}$. □

Lemma 5.18 *Let S be a taut surface with $\chi(S)=0$, then any curve $c\in\mathcal{C}$ is one of the following*:

(1) $c\in\mathcal{C}_{2,0}\cup\mathcal{C}_{1,2}$.

(2) $\mathfrak{J}(c)=4$, *ie* $c\in\mathcal{C}_{4,0}\cup\mathcal{C}_{2,2}\cup\mathcal{C}_{0,4}$.

(3) c *contains a limb* $\kappa\in\mathcal{K}$ *and has* $\mathfrak{J}(c)=\mathfrak{J}(\kappa)+2$.

(4) c *is the union of two limbs* $\kappa_1,\kappa_2\in\mathcal{K}$.

Moreover, *the cores of arcs in* $\mathcal{K}_{3,0}$ *are vertebrae of their abutting curves.*

Proof By Lemma 5.15 and 5.16 each curve $c\in\mathcal{C}$ must have $\chi'(c)=0$. It follow from the definition of χ' that the above are the only cases in which $\chi'(c)=0$.

By Remark 5.13 and Case 1 of the proof of Lemma 5.16, if c contains an arc $\kappa\in\mathcal{K}_{3,0}$ whose core is not a vertebra of the abutting curve c' then $\chi'(c)<0$. □

In Table 1 we summarize the possible sets of curves with $\chi'=0$ and assign them names.

6 Atoroidal and unannular

In this section we prove that if the link L has a diagram which satisfies the conditions of Theorem A, then its complement does not contain essential annuli or tori (in particular $\chi(S) = 0$). Let S denote such a 2-torus or annulus. After an isotopy, if need be, we may assume that S is taut. We first need the following technical lemmas.

Claim 6.1 *The following three configurations for curves $c \in \mathcal{C}$ are impossible*:

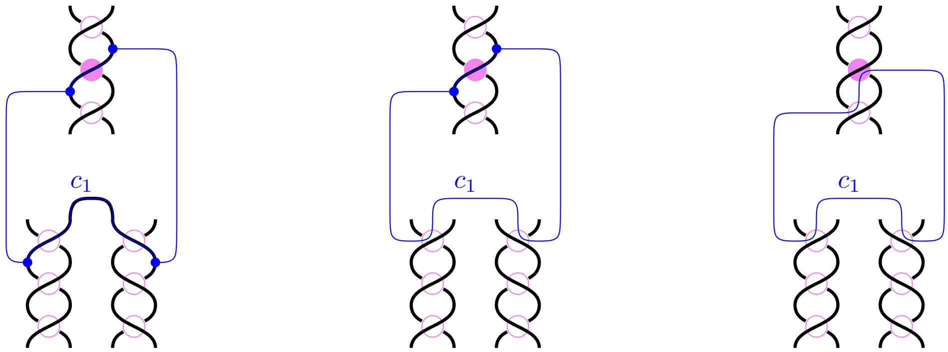

where the bubble marked in pink is nonextremal.

Proof We argue simultaneously that the three configurations are impossible. In each of these cases, let c_2 (marked in orange) be the depicted curve abutting c_1. The limb of c_2 that is shown here has three joints:

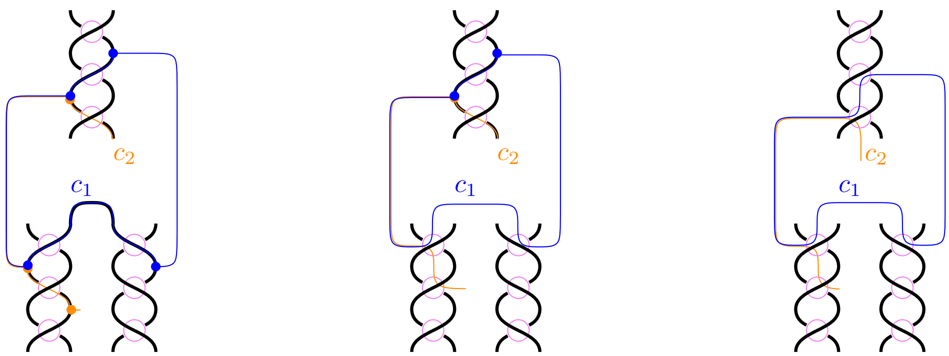

None of these joints belongs to a limb in $\mathcal{K}$: in all cases, the curve c_1 is not in $\mathcal{C}_{2,0}$ or $\mathcal{C}_{1,2}$ nor a rib with a vertebra. By Lemma 5.18, it follows that $\mathfrak{J}(c_2) = 4$. Thus the only way that c_2 can close up is in Figure 7. Let c_3 be the depicted curve abutting c_1. In the two left figures, one sees, as before, that $\mathfrak{J}(c_3) = 4$. In the figure on the right, c_3 is in $\mathcal{K}_{4,0} + 2, 0$ in the notation of Table 1: Indeed, c_3 cannot have $\mathfrak{J}(c_3) = 4$, as otherwise it bounds a twist reduction subdiagram. Thus, c_3 must contain an arc of $\mathcal{K}$. By elimination of the possibilities in Table 1, c_3 must be in $\mathcal{K}_{4,0} + 2, 0$. Thus, in all cases, c_3 can close only after passing through an additional twist region as shown in Figure 8. Thus, taking into account all

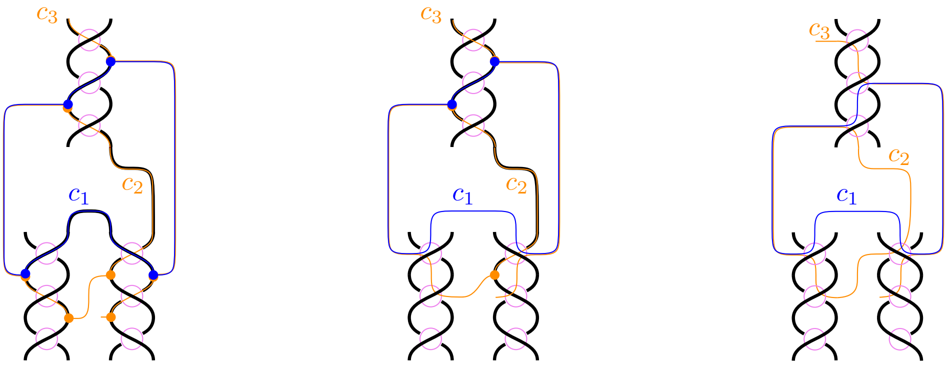

Figure 7: Proof of Claim 6.1. Second figure.

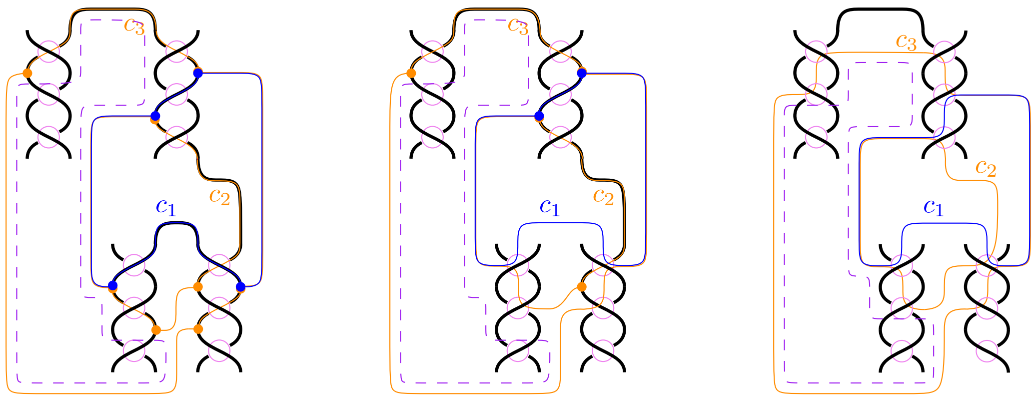

Figure 8: Proof of Claim 6.1. Third figure.

possible configurations of the curves c_2 and c_3 determined by the stated configurations of the c_1 curves, the diagrams are seen to contained a closed curve depicted by the dashed curves in the figures. Each of the dashed curves bounds a twist-reduction subdiagram. This contradicts the assumption that the diagrams are twist reduced, which finishes the proof of the claim. □

Lemma 6.2 *If a curve $c \in \mathcal{C}$ contains a bone τ connecting two turns of c then one of the following holds*:

(1) *the curve $c \in \mathcal{C}_{2,0}$*,

(2) *the curve c is a rib*, *or*

(3) *the $\circ$-bone τ meets the width edge of both twist regions.*

In particular, *c cannot have three consecutive turns.*

Proof Let τ be a bone connecting two turns of c it is therefore an $\circ$-bone. Assume in contradiction that τ and c do not satisfy any of (1)–(3) of the lemma. That is, c is not a curve in $\mathcal{C}_{2,0}$ nor a rib, and τ does not meet the width edge of both twist regions. There are two cases to consider depending on whether τ meets a width edge or not.

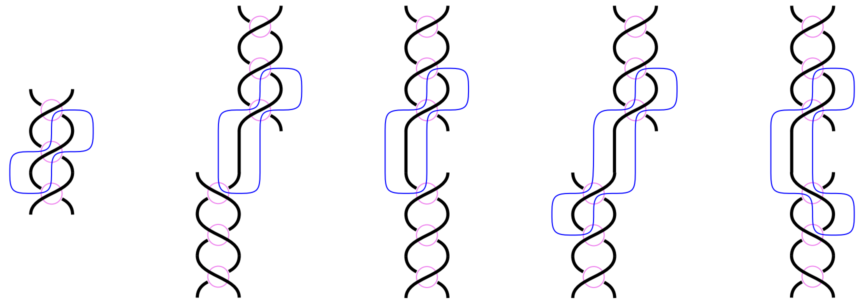

Figure 9: The five configurations of good curves which are not in $\mathcal{C}_{2,0}$.

If τ meets a width edge, then τ is a vertebra, ie it meets the length edge of one twist box and the width of the other. If this occurs set $c_0 = c,\ \tau_0 = \tau$. Since c is assumed not to be a rib, it follows from Lemma 5.6 that there exist curves $c_1, \dots, c_n$, limbs $\kappa_1, \dots, \kappa_n$, and vertebrae $\tau_1, \dots, \tau_{n-1}$ so that the terminal layer c_n has $\chi_+(c_n) < 0$. Moreover, note that the limb κ_n is not in $\mathcal{K}_{3,0}$ as otherwise by the uniqueness property, assured in Lemma 5.6, the "initial" layer curve c_0 must be a curve in $\mathcal{C}_{2,0}$ of type (i). This implies that κ_n does not meet any limb of $\mathcal{K}$. As otherwise, as in the proof of Lemma 5.11, one can prove that κ_n and the limb it meets must be equal. However, by Lemma 5.18, there is no curve, with $\chi' = 0$, which has three $\circ$-joints that do not belong to a limb of $\mathcal{K}$.

If τ does not meet a width edge, then τ meets the length edge of both twist regions. It follows that the curve c' abutting c along τ has two wiggles which are connected by τ. The curve c' cannot be in $\mathcal{C}_{4,0}$ as otherwise it bounds a twist-reduction subdiagram. By Lemma 5.18, one of the wiggles must meet a limb $\kappa \in \mathcal{K}$. Since τ is a core of c', it must be the core κ. It follows that $\kappa \in \mathcal{K}_{4,0}$ and that $c \in \mathcal{C}_{2,0}$ is of type (ii), in contradiction to our assumption.

In both cases, whether τ meets a width edge or not, we arrived at a contradiction. Hence, c must satisfy one of (1)–(3).

Finally, if c has three consecutive turns then c is not a rib nor a curve in $\mathcal{C}_{2,0}$. One of the two bones between the turns of c must meet a length edge and a width edge, contradicting (3). □

Definition 6.3 A curve $c \in \mathcal{C}$ is *good* if it bounds on $P^\pm$ exactly one component of $L \cap P^\pm$. I.e., it is either in $\mathcal{C}_{2,0}$ as depicted in Figure 5 (i) and (ii), or a curve in one of the forms shown in Figure 9.

We will say that c is good of type (I)–(V), accordingly. Otherwise, c is called *bad*.

Remark 6.4 Under the assumption that the diagram is prime and contains at least two twist regions the twist regions in each of the subfigures (II)–(V) of Figure 9 are distinct, as otherwise there is an arc of L connecting a twist region to itself, resulting in a nonprime subdiagram.

Remark 6.5 If S is a boundary parallel torus, then its intersection curves are good. A key observation is that the converse holds. That is, if all the curves of intersection of S with P are good then S is a

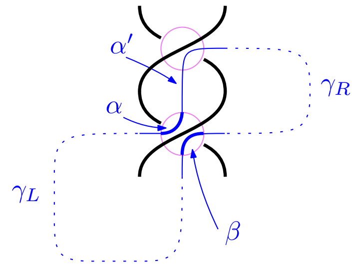

Figure 10: A curve c that meets a bubble twice.

boundary parallel torus: Consider a curve $c \in \mathcal{C}$; c is good and hence bounds on $P^{\pm}$ a unique component ℓ_c of $L \cap P^{\pm}$. When c meets a bubble B, there is a saddle of S bounded by B which meets c and two other curves c_1, c_2, and the component of $L \cap B$ that meets ℓ_c also meets ℓ_{c_1} and ℓ_{c_2}. Thus, the obvious isotopies from disks on S bounded by curves $c \in \mathcal{C}$ to ℓ_c can be glued together to form an isotopy of S to a component of L. Therefore, our goal in the next claims is to show that the curves of intersection of a taut surface S with $\chi(S) = 0$ are good.

Lemma 6.6 *If a curve $c \in \mathcal{C}$ passes through a bubble more than once, then c is good.*

Proof Let c meet the bubble B_1 more than once. By Lemma 3.9(5) it can do so only in two opposite $\circ$-joints, α, β. Therefore, at least one of those $\circ$-joints, say α, is part of a wiggle α' of c. Hence, α' meets an adjacent bubble B_2. Note that $c \smallsetminus (\alpha' \cup \beta)$ consists of two arcs connecting α' and β as depicted in Figure 10. Let γ_R, γ_L be the dotted subarcs of c on the right and left of the figure, respectively. The argument is divided into cases according to Table 1:

(1) The curve c contains three $\circ$-joints, hence it is not in $C_{2,0}$, $C_{2,2}$ or $C_{0,4}$.

(2) If $c \in \mathcal{C}_{4,0}$, then the subarc γ_R of c has no joints while γ_L has one $\circ$-joint. Hence c is good of type (I), (II) or (III).

(3) Since the three $\circ$-joints of c in T are not part of the same limb in $\mathcal{K}_{3,0}$ nor $\mathcal{K}_{4,0}$, then c cannot be in $\mathcal{K}_{3,0} + 0, 2$ or in $\mathcal{K}_{4,0} + 0, 2$ (See Table 1).

(4) The curve c cannot be in $\mathcal{K}_{4,0} + \mathcal{K}_{4,0}$: Otherwise β is part of a wiggle β' of c. The wiggle α' (resp. β') is part of a limb $\alpha'' \in \mathcal{K}_{4,0}$ (resp. $\beta'' \in \mathcal{K}_{4,0}$). Since each limb of $\mathcal{K}_{4,0}$ has a core, the bubble B_2 must be extremal. Then, the subarc γ_R of c contains the other wiggle of α''. The closed curve which is the union of γ_R and an arc on the boundary of the twist region intersects the link diagram twice, and both subdiagrams bounded by it are nontrivial. This contradicts the assumption that the diagram is prime.

(5) A similar argument shows that c cannot be in $\mathcal{K}_{2,1}$+$\mathcal{K}_{2,1}$.

(6) The curve c cannot be in $\mathcal{K}_{2,1} + 1, 1$: Otherwise, α' is the wiggle of some $\alpha'' \in \mathcal{K}_{2,1}$ and β is a turn. Beside α' and β, c has a ∂-bone on the subarc γ_L, and no joints on γ_R. Since $\alpha'' \in \mathcal{K}_{2,1}$ it abuts some $c_0 \in \mathcal{C}_{1,2}$. Hence, $c \cap L$ and $c_0 \cap L$ share endpoints. It follows that the union $(c \cap L) \cup (c_0 \cap L)$ is

a component of L passing over at most two wiggles of the diagram (at $c \cap L$) and under at most two wiggles (at $c_0 \cap L$). This contradicts the assumption that L is 3-highly twisted.

(7) If the curve c is in $\mathcal{K}_{4,0} + 2, 0$ then c is good of type (V): If β is part of a wiggle β' of c, then at most one of α' and β' is part of limb in $\mathcal{K}_{4,0}$. Without loss of generality, assume α' is a wiggle of a limb $\alpha'' \in \mathcal{K}_{4,0}$. Then, B_2 is extremal, and the subarc γ_R contains the other wiggle of α''. The curve which is the union of γ_R and an arc on the boundary of the twist region intersects the link diagram twice, in contradiction to the assumption that the diagram is prime. If β is a turn, then B_1 is extremal, and the wiggle α' is part of a limb $\alpha'' \in \mathcal{K}_{4,0}$. This limb abuts a curve $c_0 \in \mathcal{C}_{2,0}$, and it follows that c is good of type (V).

(8) Finally, if the curve c is in $\mathcal{K}_{3,0} + \mathcal{K}_{3,0}$ then c is good of type (IV): The wiggle α' is a wiggle of some limb $\alpha'' \in \mathcal{K}_{3,0}$. If β is part of a wiggle β' of c, then β' is a wiggle of some other limb $\beta'' \in \mathcal{K}_{3,0}$. It follows that each of γ_R, γ_L contains exactly one $\circ$-joint, which is impossible. If β is a turn, then it is the turn of some limb β'' in $\mathcal{K}_{3,0}$. As the core of β'' meets the width of the twist region, its wiggle must be on γ_L. Similarly, the turn of α'' must be on γ_L as well. This implies that γ_R does not contain any joints. If the turn of α'' and the wiggle of β'' are in two different twist regions then the curve abutting (both of) their cores contains three turns. However, this curve is a nonterminal layer curve (in the sense of Lemma 5.6), and those contain at most two turns. Thus, the turn of α'' and the wiggle of β'' are in the same twist region T'. Each of α'' and β'' meets an extremal bubble of T'. Then only option for them to close up is if they meet the same extremal bubble of T'. It follows that c is good of type (IV). □

Proposition 6.7 *All curves in $\mathcal{C}$ are good or in $\mathcal{C}_{0,4}$.*

In the proof of the proposition, we will assume in contradiction that such a curve exists. The proof will follow from the next four lemmas.

Lemma 6.8 *Assume that there are bad curves which are not in $\mathcal{C}_{0,4}$. Let c be an innermost bad curve in P^+ which is not in $\mathcal{C}_{0,4}$. Let D be the disk bounded by c. Then the curve c does not turn or wiggle through a twist region T which has a bubble contained in D.*

Proof **Assume *c* turns at *T*** Let B be the extreme bubble in a twist region T through which c turns. Since the diagram is 3-highly twisted T contains at least two more bubbles let B' be the bubble adjacent to B in T. By assumption B' is contained in the disk D. Consider the curve c' whose $\circ$-joint is opposite to the $\circ$-joint of c in B. Since c is innermost, the curve c' is good. It must be of good type (I) as in this configuration:

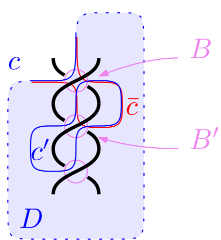

The curve $\bar{c}$ abutting both c and c', passes through the bubble B' twice. Hence, by Lemma 6.6, $\bar{c}$ is good. By the definitions, it cannot be in $\mathcal{C}_{2,0}$ nor good of type (I). If $\bar{c}$ is good of type (II) or (III) it has a turn at a bubble B'', then c passes twice through B'' which by Lemma 6.6 contradicts the assumption that c is bad. If $\bar{c}$ is good of type (IV) or (V) then it meets an extremal bubble B''. The curve c turns at B'' and hence belongs to $C_{2,0}$ which again contradicts the assumption that c is bad.

Assume c wiggles through T The curve c wiggles through the bubbles B_1, B_2. Let B_0 be a bubble of $T \cap D$ so that B_0, B_1, B_2 are consecutive, as in:

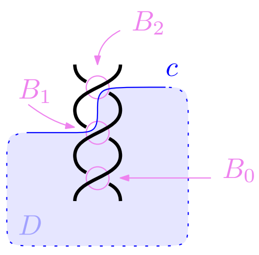

Consider the curve c' whose $\circ$-joint is opposite to the $\circ$-joint of c in B_1. The curve c' is contained in D and wiggles through T passing through the bubbles B_0, B_1:

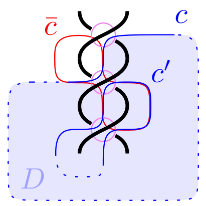

By assumption c' must be good, and so it wiggles through T and then returns to T, passing through B_0, B_1, B_0 in that order. By Lemma 3.9(5), the two $\circ$-joints of c' in B_0 are opposite sides of the same saddle. Next, consider the curve $\bar{c}$ abutting c' along the two $\circ$-bones of c' connecting B_0 and B_1. The curve $\bar{c}$ passes through B_1 twice. Hence, it is good by Lemma 6.6. It must be of type (I) and in addition passes through B_2. It follows that c abuts $\bar{c}$ along the two $\circ$-bones of $\bar{c}$ connecting B_1 and B_2. Hence, c passes through B_2 twice, and by Lemma 6.6 c is good, contradicting the assumption. □

Lemma 6.9 *Assume that there are bad curves which are not in $\mathcal{C}_{0,4}$. Let c be an innermost bad curve in P^+ which is not in $\mathcal{C}_{0,4}$. Let D be the disk bounded by c. Then the curve c does not wiggle through a twist region.*

Proof Assume that c wiggles through a twist region T. By Lemma 6.8, the disk D does not contain a bubble of T. The curve c wiggles extremely through the twist region by passing through two bubbles B_0, B_1, where B_0 is extremal. By Lemma 6.6, c meets the bubble B_0 once.

The curve c' turning at B_0 is good by choice of c. Therefore, $c' \in \mathcal{C}_{4,0}$ is good of type (II) or (III) or $c' \in \mathcal{C}_{2,0}$ of type (i) or (ii) (as in Lemma 5.1); see Figure 11.

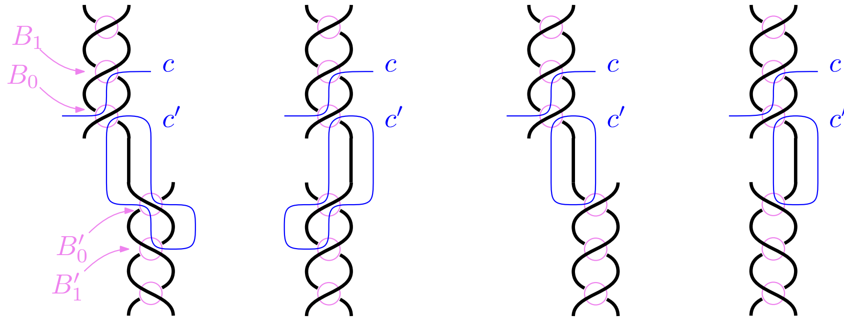

$c' \in \mathcal{C}_{4,0}$ $c' \in \mathcal{C}_{2,0}$

Figure 11: Proof of Lemma 6.9. The four configurations of c'.

Let $T' \neq T$ be the other twist region which c' meets, let B'_0 denote the extremal bubble in T' through which c' passes, and let B'_1 be its adjacent bubble.

Case 1 If $c' \in \mathcal{C}_{4,0}$ (ie as depicted in the left two subfigures in Figure 11), then consider the curve $\bar{c}$ abutting c and c' (shown in orange in subsequent figures). None of the bubbles of $\bar{c}$ belongs to an arc of $\mathcal{K}$. Therefore, $\bar{c} \in \mathcal{C}_{4,0}$, and it follows that it must close up as shown in the dotted curves here:

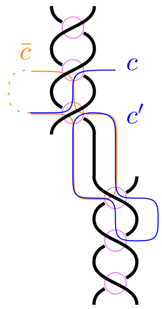

As c must follow the dotted bone of $\bar{c}$, we see that c passes through the bubbles B_1 twice. By Lemma 6.6. This contradicts the assumption that c is bad.

Case 2 Let $c' \in \mathcal{C}_{2,0}$ (ie as depicted in the right two subfigures of Figure 11) and assume that c *does not* meet B'_0. Consider, now, the curve c'' whose $\circ$-joint in B'_0 is opposite to that of c'. By the choice of c, the curve c'' is good. It must be good of type (I). And the configuration is as depicted here:

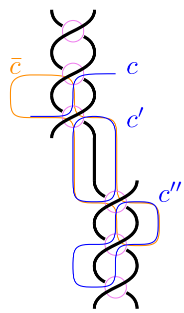

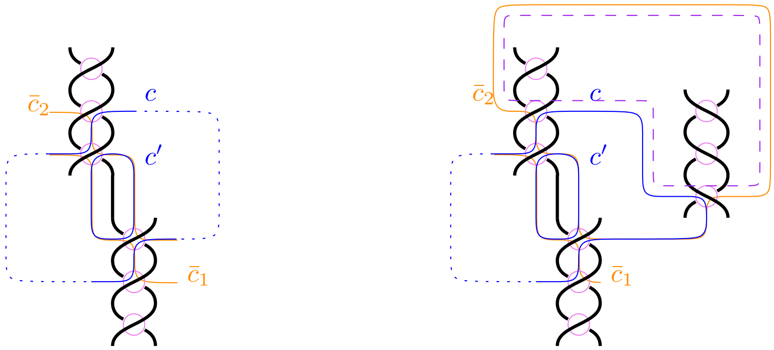

Figure 12: Subcase 3.1.

Considering the curve $\bar{c}$ abutting all of c, c', c'', we see that it must be good by Lemma 6.6 of type (IV) and (V) respectively. As in Case 1, it follows that c meets B_1 twice contradicting the assumption that c is bad.

Case 3 Assume that $c' \in \mathcal{C}_{2,0}$ of type (i) and c *does meet* B'_0 (as in the third, counted from the left, subfigure of Figure 11). In this situation are three subcases to consider:

(1) c wiggles through T' at the bubbles B'_0 and B'_1.

(2) c turns at B'_0.

(3) $c \cap L$ meets the bubble B'_0.

Subcase 3.1 The curve c wiggles through T' and through the bubbles B'_0 and B'_1. After passing through B_1, the curve c must exit T at its right length edge and enter T' on its right length edge before meeting B'_0. Otherwise the curve c would be forced to pass through a bubble twice in contradiction to Lemma 6.6. Thus, the curve c is as in Figure 12, left. If $c \in \mathcal{C}_{4,0}$ then we get a twist-reduction subdiagram, in contradiction to the assumption. Thus, by Lemma 5.18, at least one of the wiggles of c, via B_0, B_1 or via B'_0, B'_1, must be part of an arc $\kappa \in \mathcal{K}$. Since the curves $\bar{c}_1, \bar{c}_2$ abutting c' are not in $C_{2,0}$ nor in $\mathcal{C}_{1,2}$ it is clear that $\kappa \notin \mathcal{K}_{4,0} \cup \mathcal{K}_{2,1}$. Hence $\kappa \in \mathcal{K}_{3,0}$. Since c has two wiggles, it must be in $\mathcal{K}_{3,0} + \mathcal{K}_{3,0}$ (as in Table 1), and each of the dotted subarcs (in Figure 12, left) must contain a turn.

Let $\kappa \in \mathcal{K}_{3,0}$ be the limb that wiggles through B'_0, B'_1. Then, c is the terminal curve of some vertebra τ in a curve in $\mathcal{C}_{2,0}$ (in the sense of Lemma 5.6). By retracing backwards, we see that the sequence of curves terminating in c starts with $c' \in \mathcal{C}_{2,0}$, then produces $\bar{c}_2 \in \mathcal{C}_{4,0}$, and then finally produce the curve c (and the limb κ). In particular, $\bar{c}_2$ is a rib, and the $\circ$-bone connecting its two turns is a vertebra. Figure 12, right, shows an example of such a configuration of curves. As one can see, there are subarcs of $\bar{c}_2$ and c that together bound a twist-reduction subdiagram which is a contradiction.

Subcase 3.2 Assume c turns at the bubble B'_0. As explained at the beginning of the previous Subcase 3.1, the curve c must be as in Figure 13.

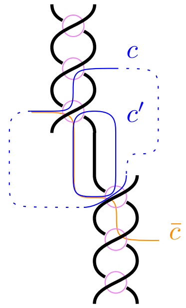

Figure 13: Subcase 3.2. The curve c' is of type (i) and c turns at B'_0.

Let $\bar{c}$ be the curve abutting c' as in Figure 13. The argument proceeds by dividing into cases according to Table 1:

(1) The curve c contains three $\circ$-joints, hence it is not in $C_{2,0}$, $C_{2,2}$ or $C_{0,4}$.

(2) The curve c is *not* in $\mathcal{C}_{4,0}$: Otherwise, c has to be a rib. The bone τ connecting the two turns cannot meet both width edges of the corresponding twist regions by Claim 6.1. Hence it is a vertebra, eg as in this figure:

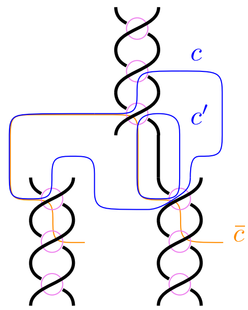

As $\bar{c}$ has at least five $\circ$-joints, by Table 1 $\bar{c}$ is in $\mathcal{K}_{3,0}+\mathcal{K}_{3,0}$, and its two cores are those of the limbs in $\mathcal{K}_{3,0}$. The core of c ending in B_0 meets the length edge of both twist regions it connects. This is impossible for a core of a limb in $\mathcal{K}_{3,0}$.

(3) The curve c cannot be in $\mathcal{K}_{4,0}+0,2$, $\mathcal{K}_{2,1}$+$\mathcal{K}_{2,1}$, or $\mathcal{K}_{4,0}+\mathcal{K}_{4,0}$ (see Table 1), since c contains a turn.

(4) The curve c cannot be in $\mathcal{K}_{3,0}+0,2$: Otherwise, the three $\circ$-joints of c are part of the same limb in $\mathcal{K}_{3,0}$. The core of such a limb connects a width edge to a length edge. This is not the case here.

(5) The curve c cannot be in $\mathcal{K}_{2,1}+1,1$ or in $\mathcal{K}_{4,0}+2,0$: Otherwise, the wiggle of c is part of a limb in $\mathcal{K}_{2,1}$ or $\mathcal{K}_{4,0}$, respectively. It follows that the curve $\bar{c}$ abutting c and c' in Figure 13 must be in $\mathcal{C}_{1,2}$ or $\mathcal{C}_{2,0}$, respectively, which is clearly not the case.

(6) Finally, the curve c cannot be in $\mathcal{K}_{3,0}+\mathcal{K}_{3,0}$: Otherwise, it follows that γ_R must contain a single wiggle. However, in this case one can close γ_R with an arc along c' to obtain a curve in P intersecting the diagram in two points contradicting the assumption that the diagram is prime.

Subcase 3.3 If $c \cap L$ meets the bubble B_0', then it is as depicted here:

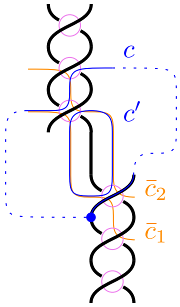

If $c \in \mathcal{C}_{2,2}$ then the left dotted line passes through no bubbles or intersection points, and we get a contradiction to the parity. Therefore, by Lemma 5.18, c must contain some arc $\kappa \in \mathcal{K}$. Clearly, κ must contain the subarc of c wiggling through T via B_0, B_1. The curve $\bar{c}_1$ is not in $\mathcal{C}_{1,2} \cup \mathcal{C}_{2,0}$ and therefore $\kappa \notin \mathcal{K}_{2,1} \cup \mathcal{K}_{4,0}$. It follows that κ is an arc in $\mathcal{K}_{3,0}$ and is the terminal layer limb of the process c', then $\bar{c}_1$, then κ, which is discussed in the proof of Lemma 5.6. If this is the case then, as in the end of Subcase 3.1, a subarc of $\bar{c}_1$ and a subarc of c bound a twist-reduction subdiagram as in the example shown here:

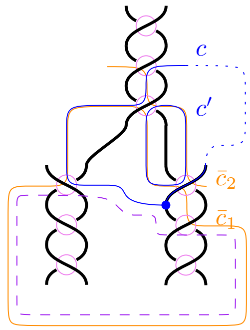

Case 4 Assume that $c' \in \mathcal{C}_{2,0}$ of type (ii) and c *does meet* B_0'. (as depicted in the rightmost subfigure of Figure 11). Let $\bar{c}_1$ be the curve abutting c as in:

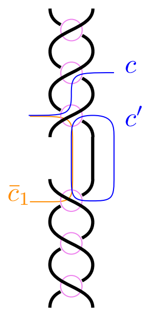

The wiggle of c passing via B_0, B_1 is not part of any arc κ in $\mathcal{K}$: If it were, then the curve $\bar{c}_1$ will either be in $\mathcal{C}_{2,0} \cup \mathcal{C}_{1,2}$ or will be the nonterminal layer curve of a process terminating in κ. Clearly, $\bar{c}_1$ is not in $\mathcal{C}_{2,0} \cup \mathcal{C}_{1,2}$. It is also not a nonterminal layer of a process defining $\mathcal{K}_{3,0}$ as in Lemma 5.6, since at any

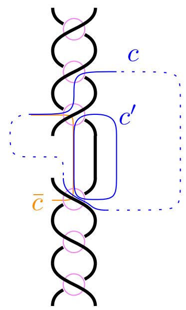

Figure 14: Subcase 4.2. The curve c' is of type (ii) and c turns at B'_0.

step of a process every curve is a rib, ie it has two turns and a wiggle, and the next step of the process abuts the $\circ$-bone connecting its the two turns, however here c does not abut the $\circ$-bone of $\bar{c}_1$ connecting its two turns.

As in the previous subcase there are three further subsubcases to consider:

(1) c wiggles through T' at the bubbles B'_0 and B'_1.

(2) c turns at B'_0.

(3) $c \cap L$ meets the bubble B'_0.

Subcase 4.1 If c wiggles through the bubbles B'_0, B'_1, the exact same argument as above shows that the subarc of c passing through B'_0, B'_1 is not a subarc of any arc in $\mathcal{K}$. It follows that $c \in \mathcal{C}_{4,0}$ and bounds a twist-reduction subdiagram,

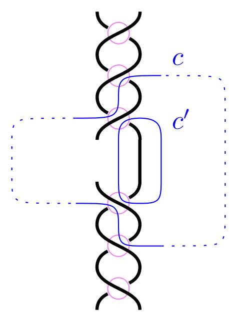

which is a contradiction.

Subcase 4.2 If c turns at the bubble B'_0. The curve c must be as in Figure 14. The argument is further divided into cases according to Table 1:

(1) The curve c contains three $\circ$-joints, hence it is not in $C_{2,0}$, $C_{2,2}$ or $C_{0,4}$.

(2) The curve c is not in $\mathcal{C}_{4,0}$: Otherwise, c has to be a rib. The bone τ connecting the two turns cannot meet both width edges of the corresponding twist regions by Claim 6.1. Hence it is a vertebra, as in Figure 15. It follows that the curve $\bar{c}$ abutting c and c' has at least three consecutive turns in contradiction to Lemma 6.2.

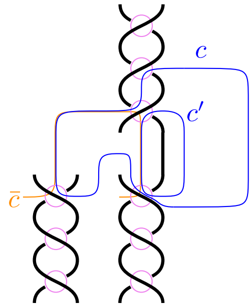

Figure 15: Subcase 4.2(2).

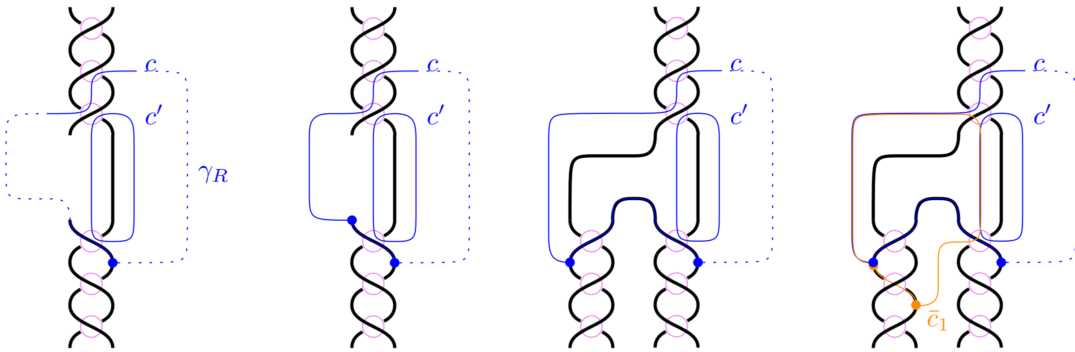

Figure 16: Subcase 4.3.

(3) The curve c cannot be in $\mathcal{K}_{4,0}+0,2$, $\mathcal{K}_{2,1}+\mathcal{K}_{2,1}$ or $\mathcal{K}_{4,0}+\mathcal{K}_{4,0}$ (See Table 1) since c contains a turn.

(4) The curve c cannot be in $\mathcal{K}_{3,0}+0,2$: Otherwise the three $\circ$-joints of c are part of the same limb in $\mathcal{K}_{3,0}$. However this would imply that the three $\circ$-joints of c are consecutive, which is impossible by the checkerboard coloring of the diagram.

(5) The curve c cannot be in $\mathcal{K}_{2,1}+1,1$ or in $\mathcal{K}_{4,0}+2,0$: Otherwise, the wiggle of c is part of a limb in $\mathcal{K}_{2,1}$ or $\mathcal{K}_{4,0}$, respectively. It follows that the curve $\bar{c}$ abutting c and c' in Figure 14 must be in $\mathcal{C}_{1,2}$ or $\mathcal{C}_{2,0}$, respectively, which is clearly not the case.

(6) Finally, the curve c cannot be in $\mathcal{K}_{3,0}+\mathcal{K}_{3,0}$: Otherwise, it follows that the curve $\bar{c}$ abutting c has three consecutive turns. This is impossible by Lemma 6.2.

Subcase 4.3 If $c \cap L$ meets the bubble B'_0, then by Table 1 c is either in $\mathcal{C}_{2,2}$, or $\mathcal{K}_{2,1}+1,1$ or $\mathcal{K}_{2,1}+\mathcal{K}_{2,1}$. It cannot be in $\mathcal{K}_{2,1}+1,1$ or $\mathcal{K}_{2,1}+\mathcal{K}_{2,1}$ since otherwise the dotted subarc γ_R has a turn or a wiggle, respectively (see Figure 16, left), which would contradict primeness. Thus, $c \in \mathcal{C}_{2,2}$.

If $c \cap L$ passes over one crossing of L, then c bounds a twist-reduction subdiagram as in Figure 16, middle left. Otherwise, we are in Figure 16, middle right. Now consider how the curve $\bar{c}_1$ abutting

c' on its left can close up. It must be as depicted in Figure 16, right. Thus, $\bar{c}_1$ must be as one of the configurations that were ruled out in Claim 6.1. □

Lemma 6.10 *Assume that there are bad curves which are not in $\mathcal{C}_{0,4}$. Let c be an innermost bad curve in P^+ which is not in $\mathcal{C}_{0,4}$. Let D be the disk bounded by c. Then $c \notin \mathcal{C}_{4,0}$.*

Proof By Lemma 6.9, c only turns. However, this is impossible by Lemma 6.2. □

Lemma 6.11 *Assume that there are bad curves which are not in $\mathcal{C}_{0,4}$. Let c be an innermost bad curve in P^+ which is not in $\mathcal{C}_{0,4}$, and let D be the disk bounded by c. Then $c \notin \mathcal{C}_{2,2}$.*

Proof Assume $c \in \mathcal{C}_{2,2}$, Since $c \smallsetminus (c \cap L)$ passes through two bubbles, the endpoints of (a small continuation of) $c \cap L$ have the same color in the checkerboard coloring of $P \smallsetminus D(L)$. Thus it is one of the following:

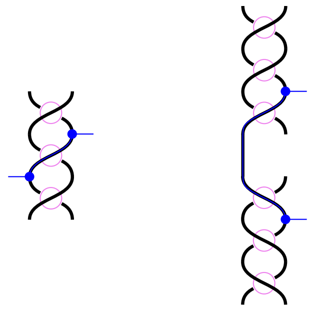

(a) (b)

By Lemmas 6.8 and 6.9, the complement $c \smallsetminus (c \cap L)$ contains two turns, in twist regions which do not contain bubbles in D. Thus, the possible configurations are:

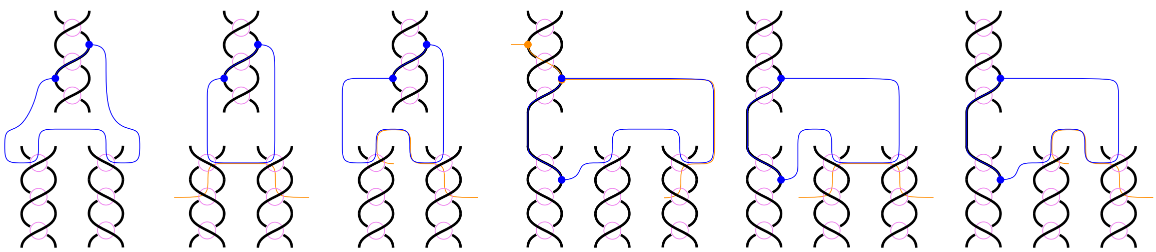

(a1) (a2) (a3) (b1) (b2) (b3)

In each of the cases, consider the curve $\bar{c}$ abutting c (a subarc of which is shown in orange).

Case (a1) is ruled out by Claim 6.1. In cases (a2), (b1), (b2), it is clear that the curve $\bar{c} \in \mathcal{C}_{4,0} \cup \mathcal{C}_{2,2}$ and bounds a twist-reduction subdiagram, which is a contradiction. Cases (a3), (b3) are impossible by Lemma 6.2. □

Proof of Proposition 6.7 Assume in contradiction that there are bad curves which are not in $\mathcal{C}_{0,4}$. Let c be an innermost bad curve in P^+ which is not in $\mathcal{C}_{0,4}$.

By the last two lemmas, c is not in $\mathcal{C}_{4,0}$ nor in $\mathcal{C}_{2,2}$. Thus, by Lemma 5.18, c must contain an arc of $\mathcal{K}$. Since every arc in $\mathcal{K}$ wiggles through some twist region, we get a contradiction to Lemma 6.9. This contradiction finishes the proof of Proposition 6.7. □

Corollary 6.12 *If the diagram of L is 3-highly twisted, connected, prime, and twist-reduced then $\mathbb{S}^3 \setminus \mathcal{N}(L)$ is atoroidal. In particular, L is prime.*

Proof Let $S \subset \mathbb{S}^3 \setminus \mathcal{N}(L)$ be an incompressible taut torus. Let $\mathcal{C}$ be the curves of intersection of S with $P^{\pm}$. Since S has no boundary, $\mathcal{C}_{0,4} = \varnothing$. By Proposition 6.7 all curves in $\mathcal{C}$ are good. We have seen in Remark 6.5 that if all curves are good then the torus S is boundary parallel.

If L was a composite knot, then the swallow-follow torus would be an essential torus in $\mathbb{S}^3 \setminus L$. □

Proposition 6.13 *If the diagram of L is 3-highly twisted, connected, prime and twist-reduced, then $\mathbb{S}^3 \setminus \mathcal{N}(L)$ is unannular.*

Proof Let S be an essential annulus. Since L is prime by Corollary 6.12, the annulus can be assumed not to have meridional boundary components. Thus, we may assume that S is taut. Let $\mathcal{C}$ be its curves of intersection with P. By Proposition 6.7 all curves in $\mathcal{C}$ are either good or in $\mathcal{C}_{0,4}$. Since S has boundary components, not all curves in $\mathcal{C}$ are good, and there is at least one curve $c \in \mathcal{C}_{0,4}$. We show that this is impossible.

If there exists a curve $c \in \mathcal{C}_{0,4}$ then the curve $\bar{c}$ abutting c has two intersection points which are not connected by an arc of $\bar{c} \cap L$ therefore $\bar{c} \in \mathcal{C}_{0,4}$. Repeating this argument shows that all the curves are in $\mathcal{C}_{0,4}$, ie $\mathcal{C} = \mathcal{C}_{0,4}$.

Case 1 There exists a curve $c \in \mathcal{C}_{0,4}$ which passes twice at the same twist region.

Denote the two connected components of $c \cap L$ by α and β. Let n be the number of crossings of T in-between α and β. We further divide the proof into subcases depending on n.

Subcase 1.0 $(n = 0)$ By Lemma 3.9(5), α and β do not meet the same bubble of T. Since we assume $n = 0$, they must meet adjacent bubbles of T. The annulus S must spiral between the strands of $L \cap T$. Thus we obtain a disk of Type 2 (as in Lemma 3.1) and hence, by the definition of $\mathcal{C}^+$ and $\mathcal{C}^-$ as in the beginning of Section 3.2 this curve does not appear in $\mathcal{C}$.

Subcase 1.1 $(n = 1)$ The tangle $L \cap T$ has two components λ_1, λ_2. Let l_1, l_2 be the corresponding components of L (possibly $l_1 = l_2$). Because $n = 1$ the arcs α and β meet the same string of $L \cap T$, say λ_1. Hence the two boundary components of S are contained in the same component l_1 of L. If $l_1 = l_2$, then there exists a curve $c' \in \mathcal{C}_{0,4}$ which meets the bridge in-between α and β, and this curve must be as in Subcase 1.0. Thus, we may assume that $l_1 \neq l_2$. Consider the disk Δ as depicted in Figure 17, left. Its interior intersects L in a single point in l_2, and its boundary is the union of an arc on S and an arc on l_1.

Figure 17: Left: the disk Δ. Right: A cross section of the twist box, the annulus S and the tori U, V.

The manifold $\mathcal{N}(S) \cup \mathcal{N}(l_1)$ has two torus boundary components U and V. See Figure 17, right. Let U be the torus that meets Δ. Let U_- be the component of $\mathbb{S}^3 \smallsetminus U$ containing l_2, and let U_+ be the other component. The torus U is incompressible in U_-, as such a compression must be on Δ and Δ does intersect l_2 once. It is also incompressible in U_+, as if a compression disk exists then since it cannot intersect l_1, it gives a compression of the annulus S, in contradiction to the incompressibility of S. By Corollary 6.12, U must be boundary parallel to either $\partial\mathcal{N}(l_2)$ or $\partial\mathcal{N}(l_1)$.

If U is parallel to $\partial\mathcal{N}(l_2)$, then since l_1 is parallel to a curve in U crossing Δ once there exists an annulus $A \subset \mathbb{S}^3 \smallsetminus L$ whose boundary is $l_1 \cup l_2$. This annulus A is incompressible, since otherwise $l_1 \cup l_2$ would be a 2-component unlink that is not linked with L, ie L is split, contradicting Corollary 5.17. The annulus A is trivially boundary-incompressible because the boundary components of A are on two different components of L. If we run the argument for A instead of S, Case 1.1 cannot occur because the boundary components of A are on two different components of L.

If U is parallel to $\partial\mathcal{N}(l_1)$, the intersection $\Delta \cap U$ is a curve on U which meets the meridian of $\mathcal{N}(l_1)$ exactly once: As if it meets it more than once, then the union $\mathcal{N}(\Delta) \cup \mathcal{N}(l_1)$ determines a once-punctured nontrivial lens space contained in $\mathbb{S}^3$, which is impossible. Thus, $\partial\Delta$ which is parallel to $\Delta \cap U$ is also parallel to l_1. Therefore, the arcs $\partial\Delta \smallsetminus l_1 \subset S$ and $l_1 \smallsetminus \partial\Delta \subset L$ bound a disk. Since the arc $\partial\Delta \smallsetminus l_1$ connects different components of S it is an essential arc, and the disk is a boundary compression for S, which is a contradiction.

Subcase 1.2 ($n \geq 2$) As the boundary of the annulus S must pass through every other bridge in T, there must be another curve of $\mathcal{C}_{0,4}$ in between α and β. By choosing an innermost such curve we are back in one of the previous cases.

Case 2 None of the curves $c \in \mathcal{C}_{0,4}$ passes twice at the same twist region. Let c_1 be a curve in $\mathcal{C}_{0,4}$. Then $c_1 \cap L$ is the disjoint union of two arcs α, β. Since all of the curves are in $\mathcal{C}_{0,4}$ and at least one curve passes over a nonextremal bubble, we may assume, by changing c_1 that one of the components, say α_1, passes over a nonextremal bubble in a twist region. The component β cannot pass over one bubble, as in this case, either c_1 passes twice in the same twist region, or defines a twist-reduction subdiagram. Thus,

β must be the arc connecting two twist regions, passing over their two extremal bubbles, and the situation is as depicted here:

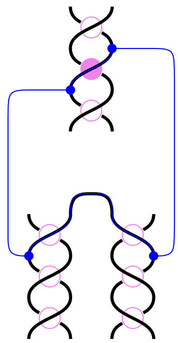

This case was ruled out in Claim 6.1. □

Remark 6.14 Subcase 1.1 ($n = 1$) in the proof of Proposition 6.13 follows also from the following well known general statement:

Nonsplit, annular atoroidal links in $\mathbb{S}^3$ are either torus knots or a link consisting of a torus knot on the "standard torus" $\mathbb{T}^2$ in $\mathbb{S}^3$ and one or both of the core curves of the solid tori components of $\mathbb{S}^3 \smallsetminus \mathcal{N}(\mathbb{T}^2)$.

For completeness we include a proof.

Proof Let $L \subset \mathbb{S}^3$ be a nonsplit and an atoroidal link in $\mathbb{S}^3$ containing an essential annulus A. If L is a knot then boundary A cuts $\partial\mathcal{N}(L)$ into two annuli A_1 and A_2. The surfaces $A \cup A_1$ and $A \cup A_2$ are tori which bound solid tori V_1 and V_2 as L is atoroidal. The two solid tori are glued to each other along A and since the result together with a regular neighborhood of L is $\mathbb{S}^3$, then by Seifert (see [13]), their complement is a regular neighborhood of a torus knot.

If L is a nonhyperbolic, nonsplit link whose exterior is atoroidal then by [14] it is a Seifert link, ie its exterior is a Seifert fiber space. Links in Seifert spaces were classified by Burde and Murasugi in [1]. They are either a connected sum of Hopf links or consist of a union of Seifert fibers in some Seifert fibration of $\mathbb{S}^3$. Atoroidal such links can contain at most three fibers. Hence the link L is a torus knot K on an unknotted solid torus $\mathbb{T}$ and the Hopf link which is the core curves of the complementing solid tori. □

Proof of Theorem A By Thurston [14], it suffices to prove that $\mathbb{S}^3 \smallsetminus \mathcal{N}(L)$ has incompressible boundary, and is irreducible, atoroidal and unannular. By Corollary 5.17 it has incompressible boundary and is irreducible, by Corollary 6.12 it is atoroidal, and by Proposition 6.13 it is unannular. □

7 Essential holed spheres in highly twisted link complements

In this section we use Theorem A to show that certain holed spheres in the complement of a highly twisted links are essential. We begin with three definitions.

Definition 7.1 Let $D(T)$ be a projection of a tangle (B,T) onto a disk $\Delta \subset P$ where $\partial\Delta$ is the simple closed curve $\gamma \subset P$ and so that the end points of the strings of T denoted by ∂T are contained in γ. We call $D(T)$ a *tangle diagram*. Let $\overline{D}(T)$ denote the reflection of $D(T)$ along P (ie the diagram with the same projection, but with reverse crossing data).

Definition 7.2 The diagram $D(T)$ is *relatively prime* (resp. *relatively twist reduced*, *relatively k-highly twisted*) if the link diagram obtained by gluing $D(T)$ and $\overline{D}(T)$ along their boundary is prime (resp. twist reduced, k-highly twisted).

Definition 7.3 A surface S in $(\mathbb{S}^3, \mathcal{L})$ is *pairwise-incompressible* if every disk D in $\mathbb{S}^3$ with $\partial D = D \cap S$, and which intersects $\mathcal{L}$ transversely in a single point, is isotopic to a disk in S by an isotopy preserving $\mathcal{L}$ setwise.

The surface S is *acylindrical* if the complement of S in $\mathbb{S}^3 \smallsetminus \mathcal{N}(\mathcal{L})$ contains no essential annuli whose boundary is on $S \cup \partial\mathcal{N}(\mathcal{L})$.

Theorem B *Let $D(L)$ be a 3-highly twisted diagram and let γ be a simple closed curve in $D(L)$ intersecting $D(L)$ transversely. Assume that both tangle diagrams bounded by γ are connected, relatively prime, relatively twist-reduced, relatively 3-highly twisted and contain at least two twist regions each. Let Σ be the sphere in $\mathbb{S}^3$ which intersects P transversely in γ, and does not intersect $\mathcal{L}$ outside γ. Then the punctured sphere $\Sigma' = \Sigma \smallsetminus \mathcal{N}(\mathcal{L})$ is incompressible, boundary-incompressible, pairwise-incompressible and acylindrical in $\mathbb{S}^3 \smallsetminus \mathcal{N}(\mathcal{L})$.*

Proof Assume in contradiction that $\Sigma' = \Sigma \smallsetminus \mathcal{N}(\mathcal{L})$ is either compressible, boundary-compressible, pairwise-compressible or not acylindrical in $\mathbb{S}^3 \smallsetminus \mathcal{N}(\mathcal{L})$.

Let B_1, B_2 be the two 3-balls that Σ bounds in $\mathbb{S}^3$, and let $E_1 = P \cap B_1,\ E_2 = P \cap B_2$ be the corresponding two disks in P bounded by γ. The induced tangle diagrams on E_1 and E_2 are assumed to be relatively prime, relatively twist-reduced and relatively 3-highly twisted. After doubling each of E_1 and E_2, as in Definition 7.2, we get two link diagrams $D(L_1), D(L_2)$ which are connected, prime, twist-reduced and 3-highly twisted. By Theorem A, the associated links $\mathcal{L}_1, \mathcal{L}_2$ are hyperbolic.

(1) If Σ' is compressible then the doubling of an innermost compressing disk $\Delta \subset B_i$ will give rise to an essential 2-sphere in $\mathbb{S}^3 \smallsetminus \mathcal{N}(\mathcal{L}_i)$.

(2) If Σ' is boundary compressible with boundary compression disk $\Delta \subset B_i$, then the doubling of Δ along $\Sigma' \cap \Delta$ results in a disk which is bounded by a component of $\mathcal{L}_i$. Hence either $\mathcal{L}_i$ is the unknot or has a split unknot component.

(3) If Σ' is pairwise boundary compressible, then the doubling of the essential disk $\Delta \subset B_i$ intersecting $\mathcal{L}$ once is a 2-sphere intersecting the boundary of $\mathcal{N}(\mathcal{L}_i)$ in two meridians. Thus $\mathcal{L}_i$ is not prime.

(4) If Σ' contains an essential annulus $A \subset B_i$ (ie Σ' is cylindrical), then $\mathcal{L}_i$ is toroidal if both boundaries of A are on Σ', or annular if one of these boundaries is on Σ' and the other on $\partial\mathcal{N}(\mathcal{L})$.

In all these cases we get that one of the links $\mathcal{L}_1, \mathcal{L}_2$ is not hyperbolic and thus a contradiction. □

References

[1] **G Burde**, **K Murasugi**, *Links and Seifert fiber spaces*, Duke Math. J. 37 (1970) 89–93 MR Zbl

[2] **M Culler**, **C M Gordon**, **J Luecke**, **P B Shalen**, *Dehn surgery on knots*, Bull. Amer. Math. Soc. 13 (1985) 43–45 MR Zbl

[3] **D Futer**, **E Kalfagianni**, **J S Purcell**, *Hyperbolic semi-adequate links*, Comm. Anal. Geom. 23 (2015) 993–1030 MR Zbl

[4] **D Futer**, **J S Purcell**, *Links with no exceptional surgeries*, Comment. Math. Helv. 82 (2007) 629–664 MR Zbl

[5] **A Giambrone**, *Combinatorics of link diagrams and volume*, J. Knot Theory Ramifications 24 (2015) art. id. 1550001 MR Zbl

[6] **C M Gordon**, **J Luecke**, *Knots are determined by their complements*, Bull. Amer. Math. Soc. 20 (1989) 83–87 MR Zbl

[7] **A Hatcher**, **W Thurston**, *Incompressible surfaces in 2–bridge knot complements*, Invent. Math. 79 (1985) 225–246 MR Zbl

[8] **M Lackenby**, *Word hyperbolic Dehn surgery*, Invent. Math. 140 (2000) 243–282 MR Zbl

[9] **T Li**, *Rank and genus of 3–manifolds*, J. Amer. Math. Soc. 26 (2013) 777–829 MR Zbl

[10] **M Lustig**, **Y Moriah**, *Are large distance Heegaard splittings generic?*, J. Reine Angew. Math. 670 (2012) 93–119 MR Zbl

[11] **W Menasco**, *Closed incompressible surfaces in alternating knot and link complements*, Topology 23 (1984) 37–44 MR Zbl

[12] **Y N Minsky**, **Y Moriah**, *Discrete primitive-stable representations with large rank surplus*, Geom. Topol. 17 (2013) 2223–2261 MR Zbl

[13] **H Seifert**, *Topologie Dreidimensionaler Gefaserter Räume*, Acta Math. 60 (1933) 147–238 MR Zbl

[14] **W P Thurston**, *The geometry and topology of three-manifolds*, lecture notes, Princeton University (1979) Available at `https://url.msp.org/gt3m`

Department of Mathematics, Technion
Haifa, Israel

`lazarovich@technion.ac.il`, `ymoriah@technion.ac.il`, `talipi@technion.ac.il`

Received: 6 September 2022 Revised: 23 July 2023

Algebraic & Geometric Topology
msp.org/agt

See inside back cover or msp.org/agt for submission instructions.

The subscription price for 2025 is US $760/year for the electronic version, and $1110/year (+$75, if shipping outside the US) for print and electronic. Subscriptions, requests for back issues and changes of subscriber address should be sent to MSP. Algebraic & Geometric Topology is indexed by Mathematical Reviews, Zentralblatt MATH, Current Mathematical Publications and the Science Citation Index.

Algebraic & Geometric Topology (ISSN 1472-2747 printed, 1472-2739 electronic) is published 9 times per year and continuously online, by Mathematical Sciences Publishers, c/o Department of Mathematics, University of California, 798 Evans Hall #3840, Berkeley, CA 94720-3840. Periodical rate postage paid at Oakland, CA 94615-9651, and additional mailing offices. POSTMASTER: send address changes to Mathematical Sciences Publishers, c/o Department of Mathematics, University of California, 798 Evans Hall #3840, Berkeley, CA 94720-3840.

AGT peer review and production are managed by EditFlow® from MSP.

PUBLISHED BY
mathematical sciences publishers
nonprofit scientific publishing
https://msp.org/

ALGEBRAIC & GEOMETRIC TOPOLOGY

Volume 25 Issue 1 (pages 1–644) 2025